

THE SPATIAL SUB-SEPARATION OF STRANGENESS FROM ANTI- STRANGENESS IN RHICs



L. Bravina, O. Panova, O. Vitiuk, E. Zabrodin

University of Oslo

H. Stocker (FIAS, Uni-Frankfurt)

Outline

- I. Motivation
- II. Thermalization in relativistic heavy-ion collisions. Statistical model of ideal hadron gas
- III. Strangeness in the central cell
- IV. Freeze-out (dN/dt) of main hadron species
- V. Spatial separation of S from anti-S :
 - in Thermal model predictions of Yields
 - directed flow for different particles
 - in Λ - $\bar{\Lambda}$ polarization
- VI. Conclusions

Dynamic Regimes

Parton distribution,
Nuclear geometry
Nuclear shadowing

Parton production &
regeneration
(or, sQGP)

Chemical freeze-out
(Quark recombination)

Jet fragmentation
functions

Hadron rescattering

Thermal freeze-out

Hadron decays

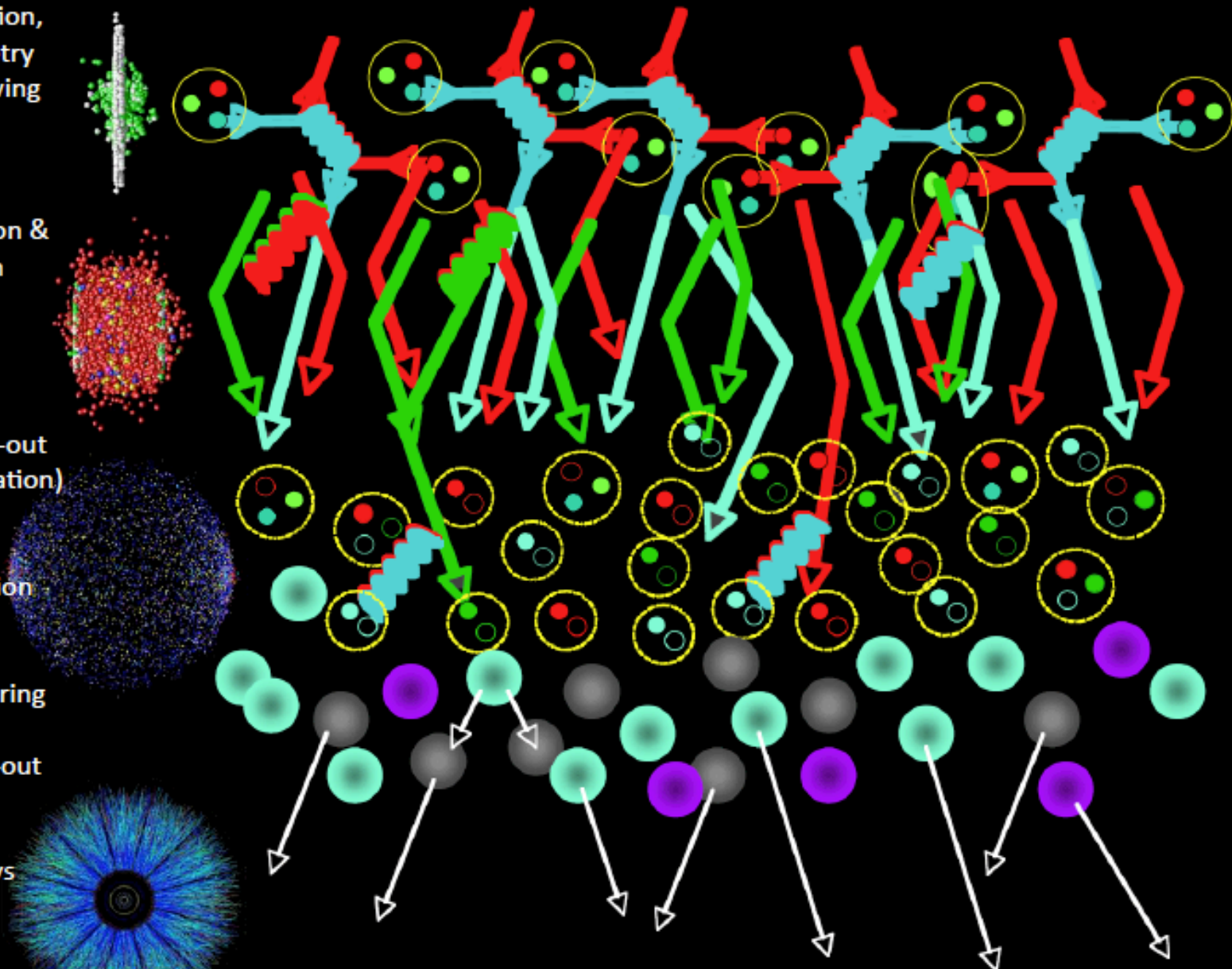
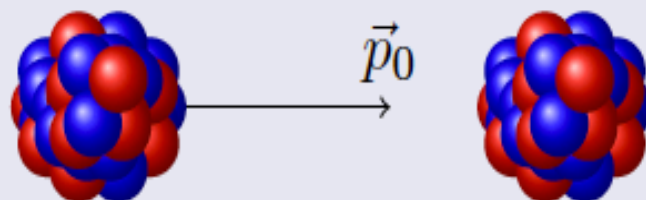


Diagram by Peter Steinberg

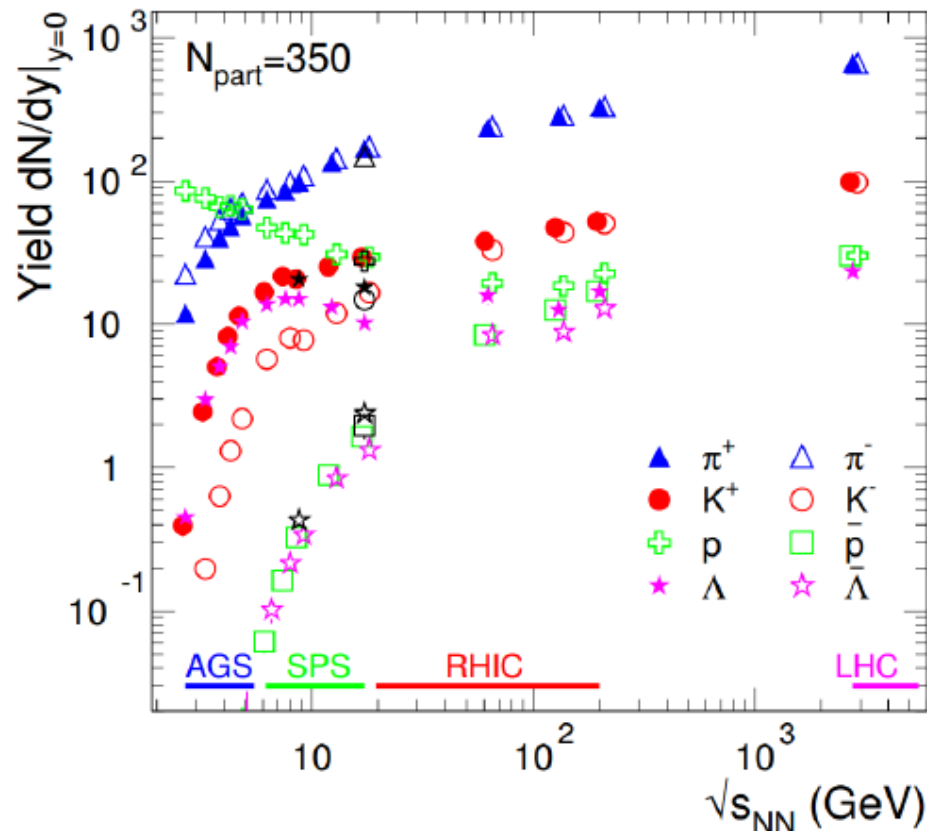
Motivation

Au+Au at $E_{lab} = 40A$ GeV and $b = 0$ fm within UrQMD



- To do the analysis of the spatio-temporal evolution of all particles in the $T - \mu_B$, $T - \mu_S$ plane and the analysis of the finally emitted particles in $x - t$ plane.
- See the spatial separation of strange particles from non strange (and of mesons from baryons).
- Find average T, μ_B, μ_S of different particles at freeze-out time.

Identified hadron yields



- Lots of particles, most newly created from the excited gluon fields ($E=mc^2$)
- Large variety of species:
 - $\pi^\pm(u\bar{d}, d\bar{u})$, $m=140$ MeV
 - $K^\pm(u\bar{s}, s\bar{u})$, $m=494$ MeV
 - $p(uud)$, $m=938$ MeV
 - $\Lambda(uds)$, $m=1116$ MeV
 - also: $\Xi(dss)$, $\Omega(sss)$, ...
- Abundancies follow mass hierarchy, except at low energies where remnants from the incoming nuclei are significant
- What do we learn?

Grand Canonical Ensemble

$$\ln Z_i = \frac{V g_i}{2\pi^2} \int_0^\infty p^2 dp \ln(1 \pm \exp(-(E_i - \mu_i)/T))$$

$$n_i = N/V = -\frac{T}{V} \frac{\partial \ln Z_i}{\partial \mu} = \frac{g_i}{2\pi^2} \int_0^\infty \frac{p^2 dp}{\exp((E_i - \mu_i)/T) \pm 1}$$

$$\mu_i = \mu_B B_i + \mu_S S_i + \mu_{I_3} I_i^3$$

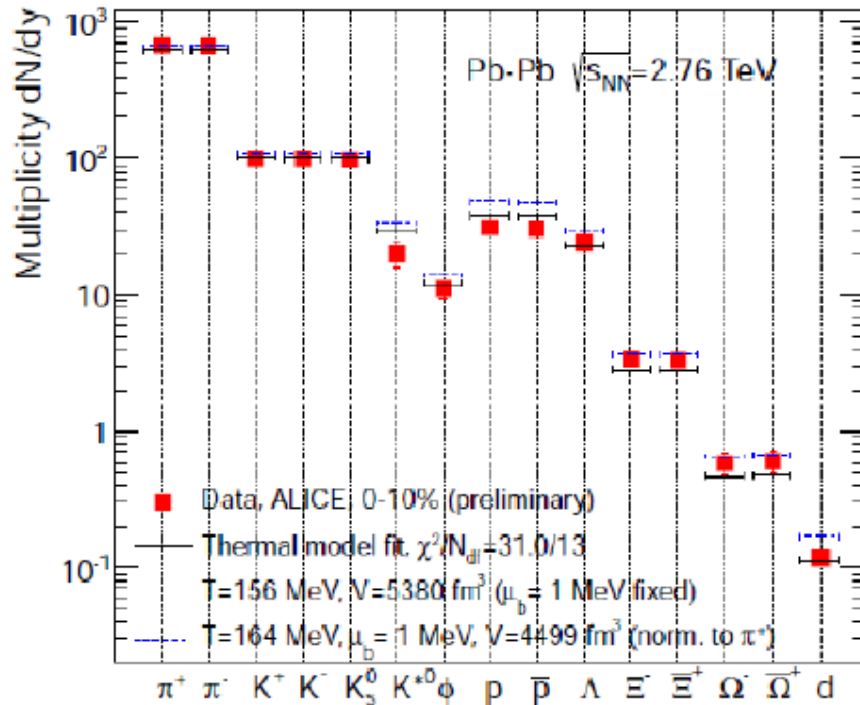
Fit at each
energy
provides
values for
 T and μ_b

for every conserved quantum number there is a chemical potential μ
but can use conservation laws to constrain:

- Baryon number: $V \sum_i n_i B_i = Z + N \rightarrow V$
- Strangeness: $V \sum_i n_i S_i = 0 \rightarrow \mu_S$
- Charge: $V \sum_i n_i I_i^3 = \frac{Z - N}{2} \rightarrow \mu_{I_3}$

This leaves only μ_b and T as free parameter when 4π considered
for rapidity slice fix volume e.g. by dN_{ch}/dy

Chemical freeze-out



- Thermal fits of hadron abundances:

$$n_i = N_i/V = -\frac{T}{V} \frac{\partial \ln Z_i}{\partial \mu} = \frac{g_i}{2\pi^2} \int_0^\infty \frac{p^2 dp}{\exp[(E_i - \mu_i)/T] \pm 1}$$

- Quantum numbers conservation

$$\mu = \mu_B B + \mu_{I3} I_3 + \mu_S S + \mu_C C$$

- Hadron yields N_i can be obtained using only 3 parameters: $(T_{\text{chem}}, \mu_B, V)$

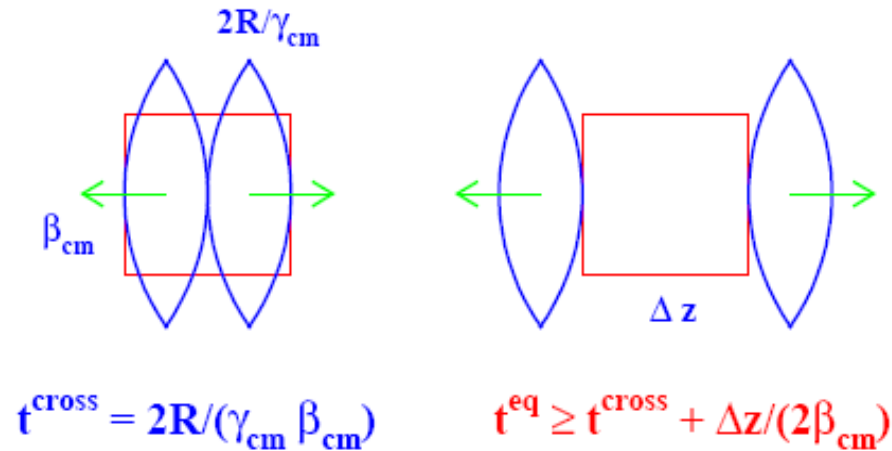
- The hadron abundances are in agreement with a thermally equilibrated system

$$T_{\text{chem}} = 155-165 \text{ MeV}$$

$$\mu_B \sim 0$$

Central cell:
Relaxation to
(local) equilibrium

Equilibration in the Central Cell



Kinetic equilibrium:

Isotropy of velocity distributions

Isotropy of pressure

Thermal equilibrium:

Energy spectra of particles are described by Boltzmann distribution

L.Bravina et al., PLB 434 (1998) 379;
JPG 25 (1999) 351

$$\frac{dN_i}{4\pi p E dE} = \frac{V g_i}{(2\pi\hbar)^3} \exp\left(\frac{\mu_i}{T}\right) \exp\left(-\frac{E_i}{T}\right)$$

Chemical equilibrium:

Particle yields are reproduced by SM with the same values of (T, μ_B, μ_S) :

$$N_i = \frac{V g_i}{2\pi^2 \hbar^3} \int_0^\infty p^2 dp \exp\left(\frac{\mu_i}{T}\right) \exp\left(-\frac{E_i}{T}\right)$$

Statistical model of ideal hadron gas

input values

output values

$$\epsilon^{\text{mic}} = \frac{1}{V} \sum_i E_i^{\text{SM}}(T, \mu_B, \mu_S),$$

$$\rho_B^{\text{mic}} = \frac{1}{V} \sum_i B_i \cdot N_i^{\text{SM}}(T, \mu_B, \mu_S),$$

$$\rho_S^{\text{mic}} = \frac{1}{V} \sum_i S_i \cdot N_i^{\text{SM}}(T, \mu_B, \mu_S).$$

Multiplicity 

Energy 

Pressure 

Entropy density 

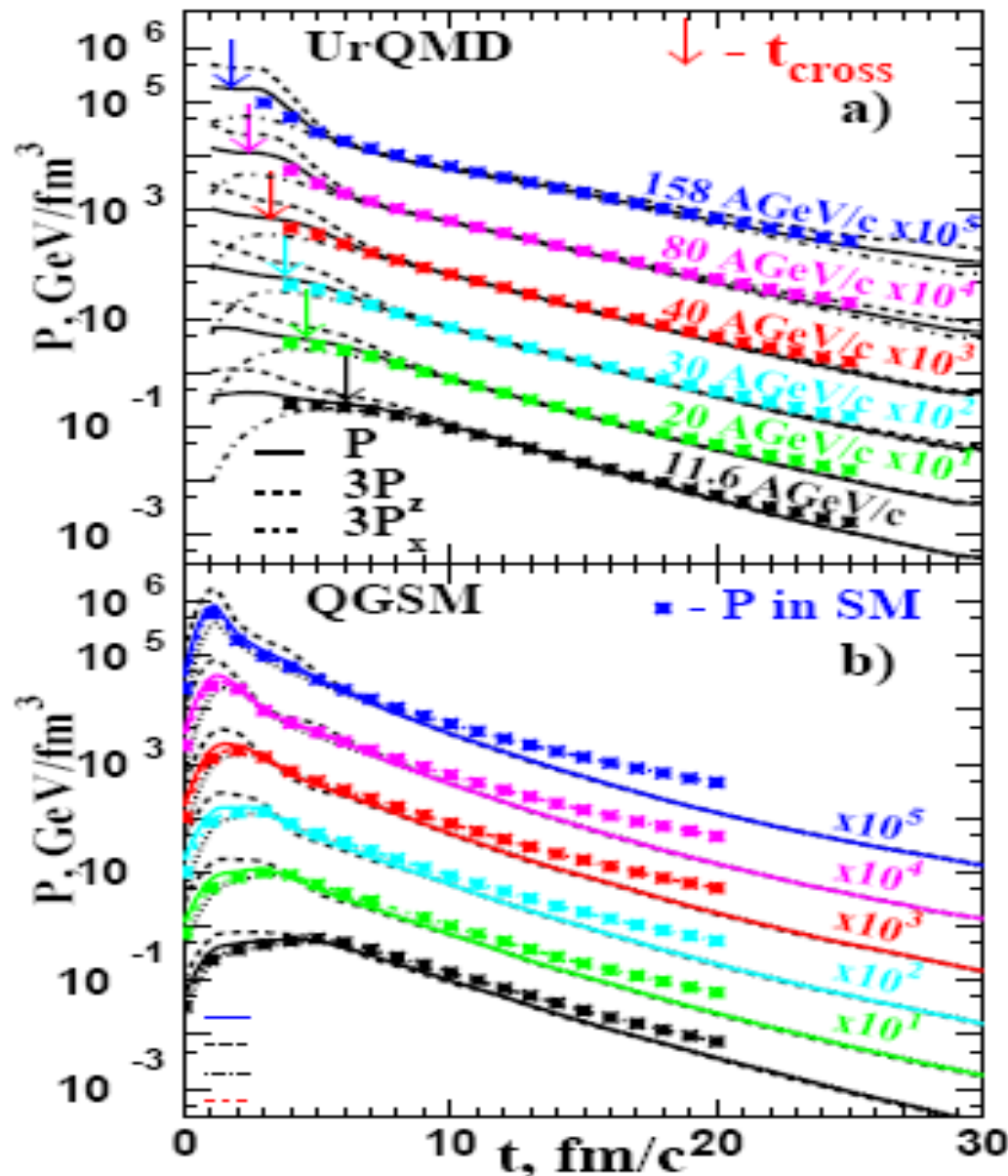
$$N_i^{\text{SM}} = \frac{V g_i}{2\pi^2 \hbar^3} \int_0^\infty p^2 f(p, m_i) dp,$$

$$E_i^{\text{SM}} = \frac{V g_i}{2\pi^2 \hbar^3} \int_0^\infty p^2 \sqrt{p^2 + m_i^2} f(p, m_i) dp$$

$$P^{\text{SM}} = \sum_i \frac{g_i}{2\pi^2 \hbar^3} \int_0^\infty p^2 \frac{p^2}{3(p^2 + m_i^2)^{1/2}} f(p, m_i) dp$$

$$s^{\text{SM}} = - \sum_i \frac{g_i}{2\pi^2 \hbar^3} \int_0^\infty f(p, m_i) [\ln f(p, m_i) - 1] p^2 dp$$

Kinetic Equilibrium



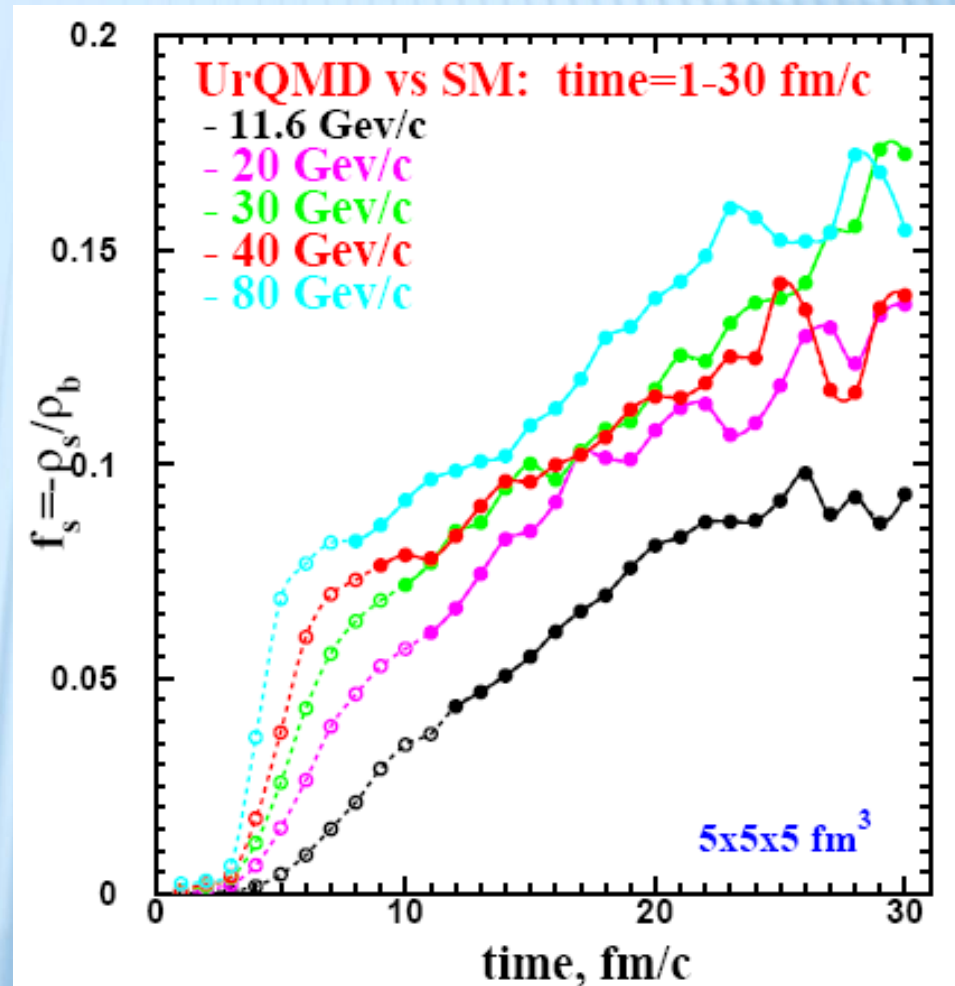
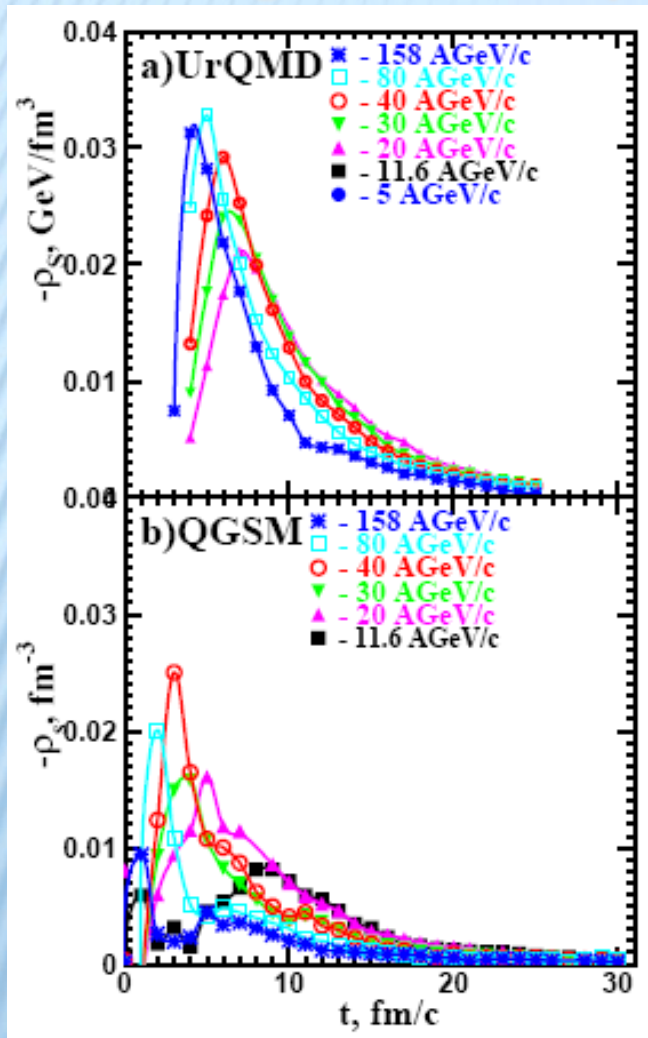
Isotropy of pressure

L.Bravina et al.,
PRC 78 (2008) 014907

Pressure becomes isotropic
for all energies from 11.6
A GeV to 158 A GeV

NEGATIVE NET STRANGENESS DENSITY

Net strangeness density in the central cell at 11 to 80 AGeV

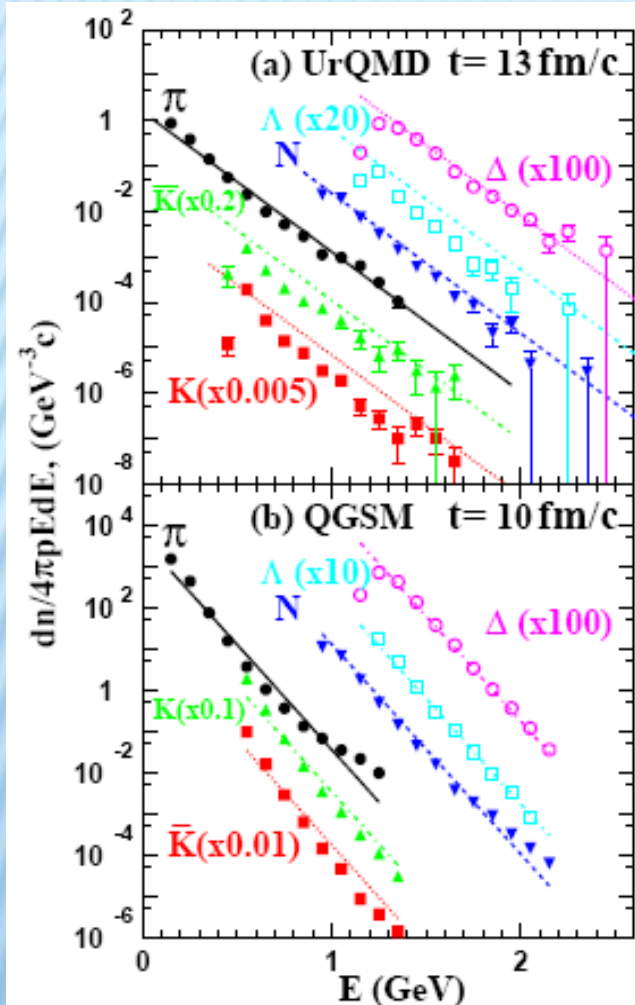


Net strangeness in the cell is negative because of different interaction cross sections for **Kaons** and **antiKaons** with **Baryons**

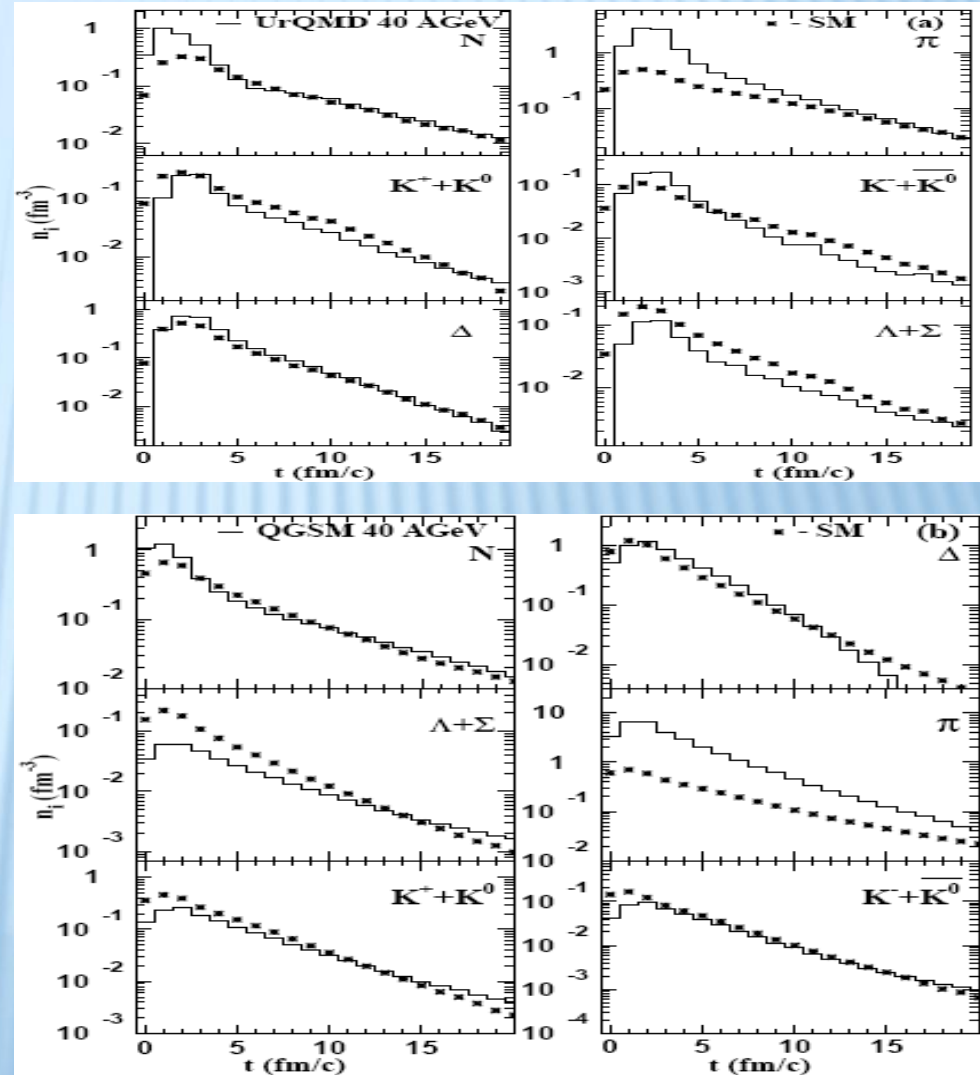
THERMAL AND CHEMICAL EQUILIBRIUM

Boltzmann fit to the energy spectra

Particle yields

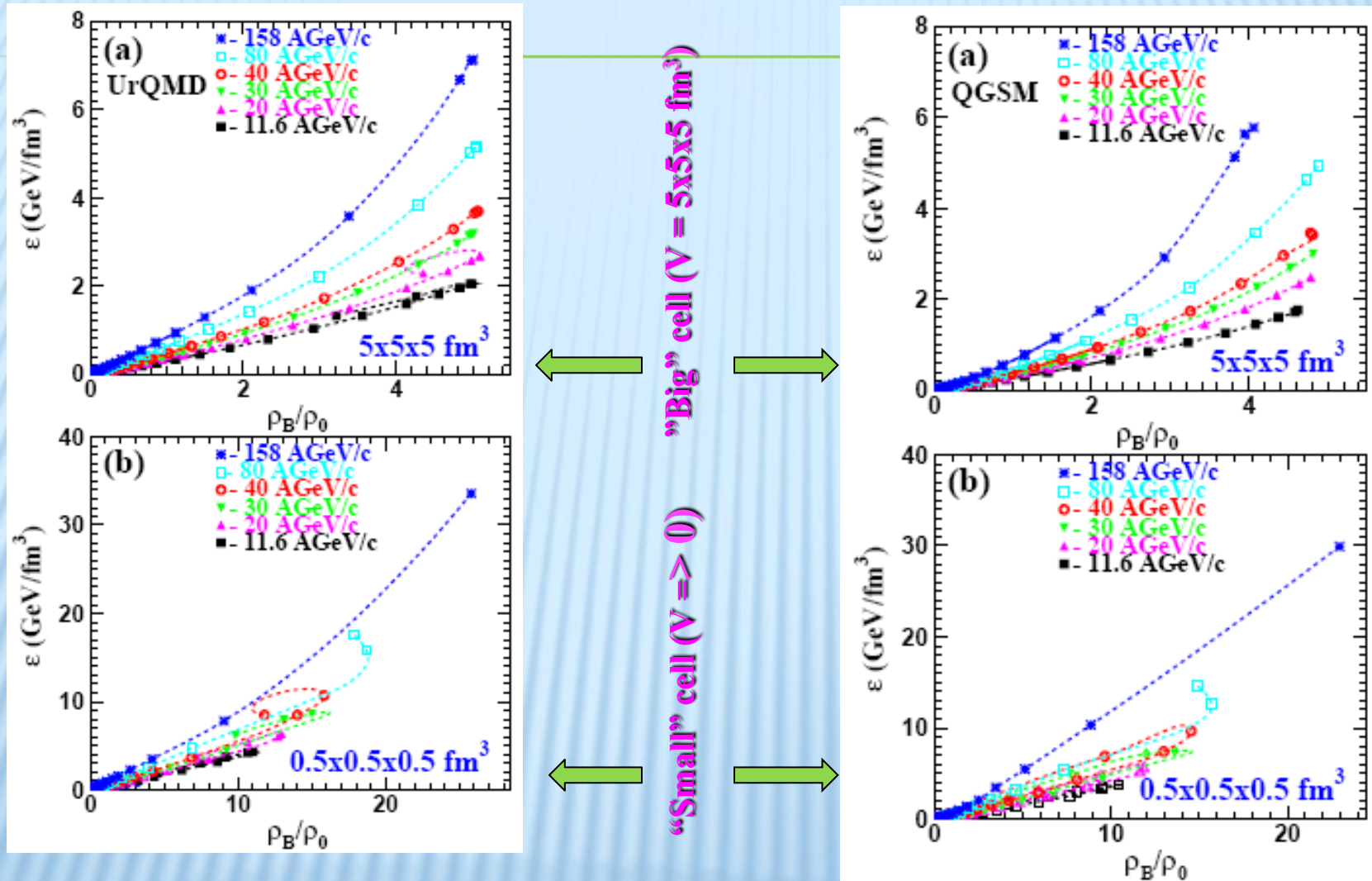


PRC 78 (2008) 014907



Thermal and chemical equilibrium seems to be reached

HOW DENSE CAN BE THE MEDIUM?

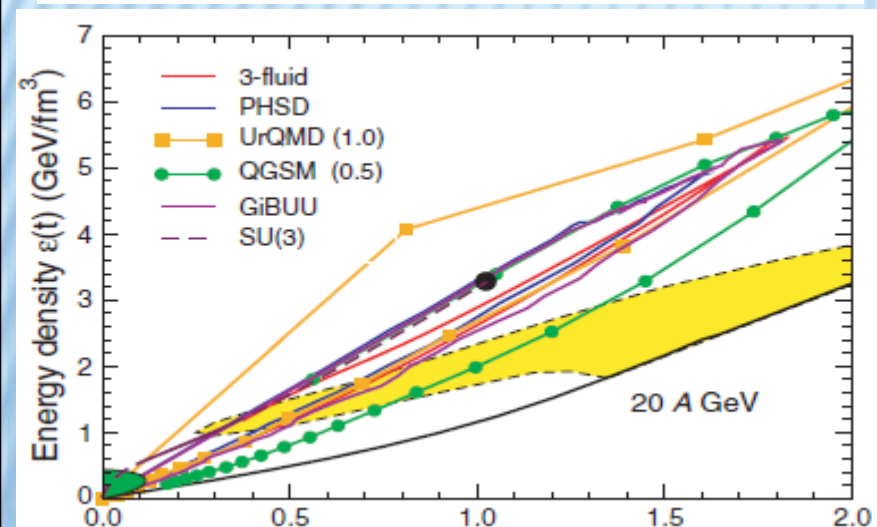
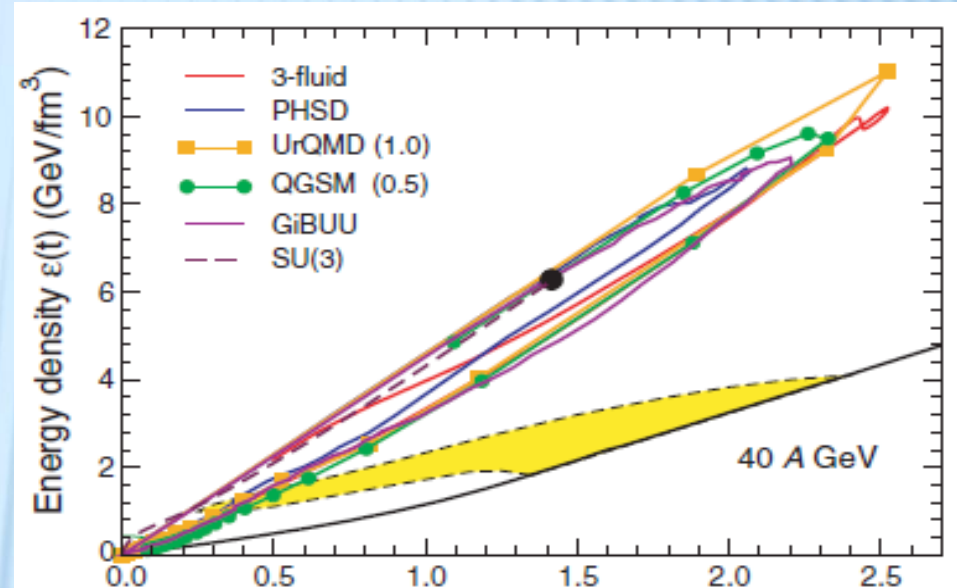
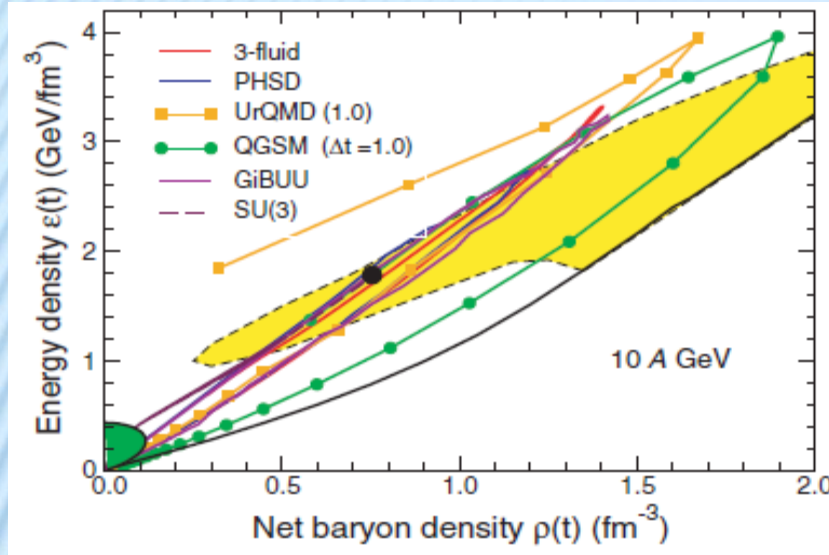


Dramatic differences at the non-equilibrium stage; after beginning of kinetic equilibrium the energy densities and the baryon densities are the same for "small" and "big" cell

COMPARISON BETWEEN MODELS

The phase trajectories at the center of a head-on Au+Au collisions

I. Arsene et al., PRC 75 (2007) 034902



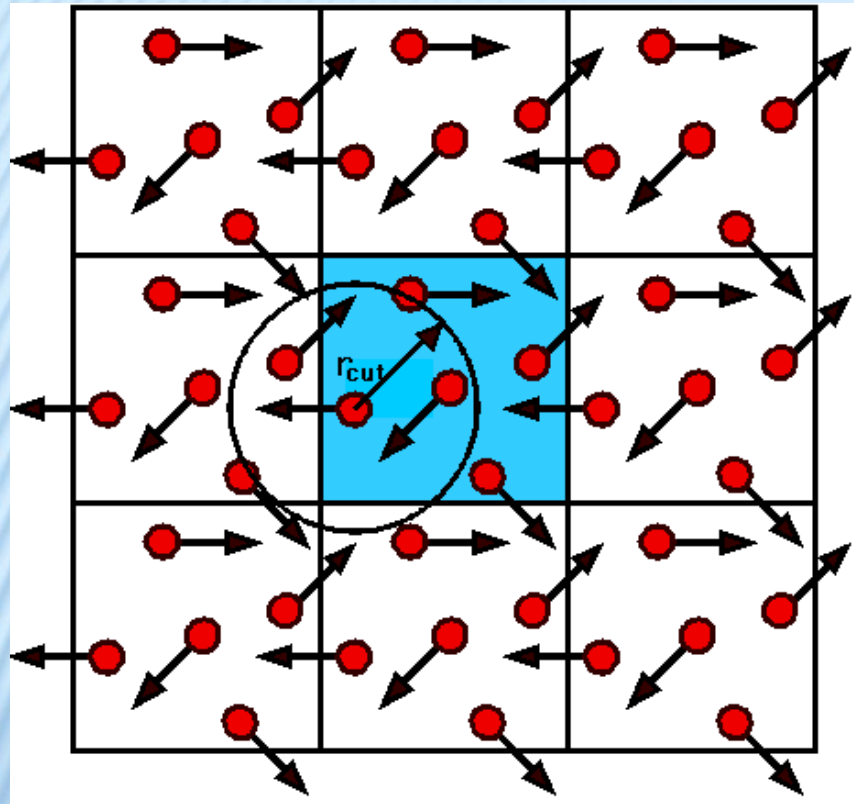
Green area : freeze-out region;
Yellow area : the phase coexistence
region from schematic EOS that has
a critical point at final density

Different models exhibit a large degree of mutual agreement

Infinite hadron gas:
a box with periodic
boundary conditions

BOX WITH PERIODIC BOUNDARY CONDITIONS

M.Belkacem et al., PRC 58, 1727 (1998)



Model employed: UrQMD
55 different baryon species
(N, Δ , hyperons and their
resonances with

$m \leq 2.25 \text{ GeV}/c^2$),

32 different meson species
(including resonances with
 $m \leq 2 \text{ GeV}/c^2$) and their
respective antistates.

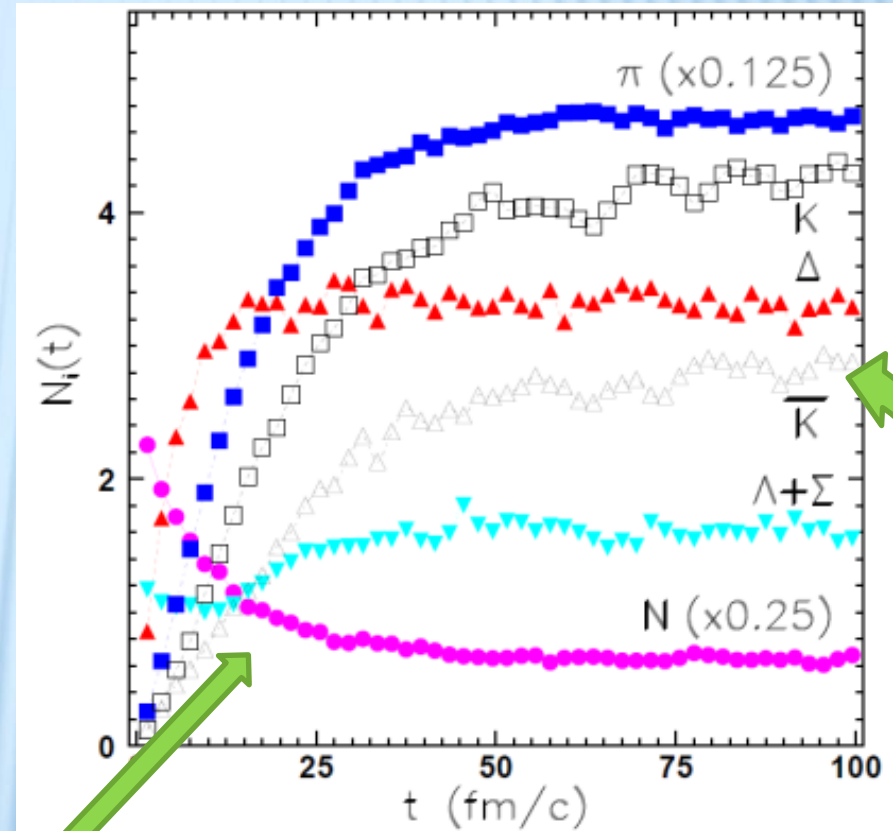
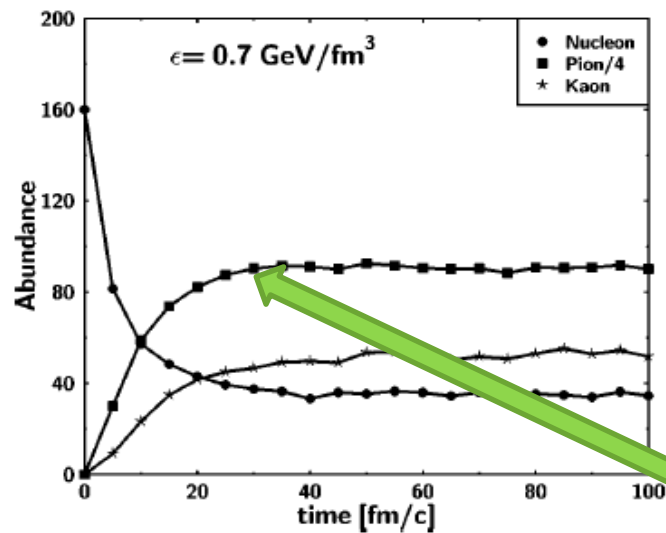
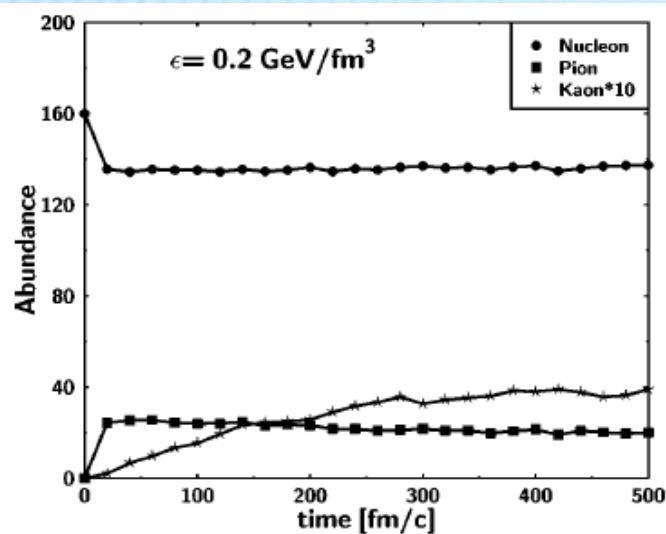
For higher mass excitations
a string mechanism is invoked.

Initialization: (i) nucleons are uniformly
distributed in a configuration space;
(ii) Their momenta are uniformly distributed
in a sphere with random radius and then
rescaled to the desired energy density.

Test for equilibrium: particle yields and energy spectra

BOX: PARTICLE ABUNDANCES

M.Belkacem et al., PRC 58, 1727 (1998)

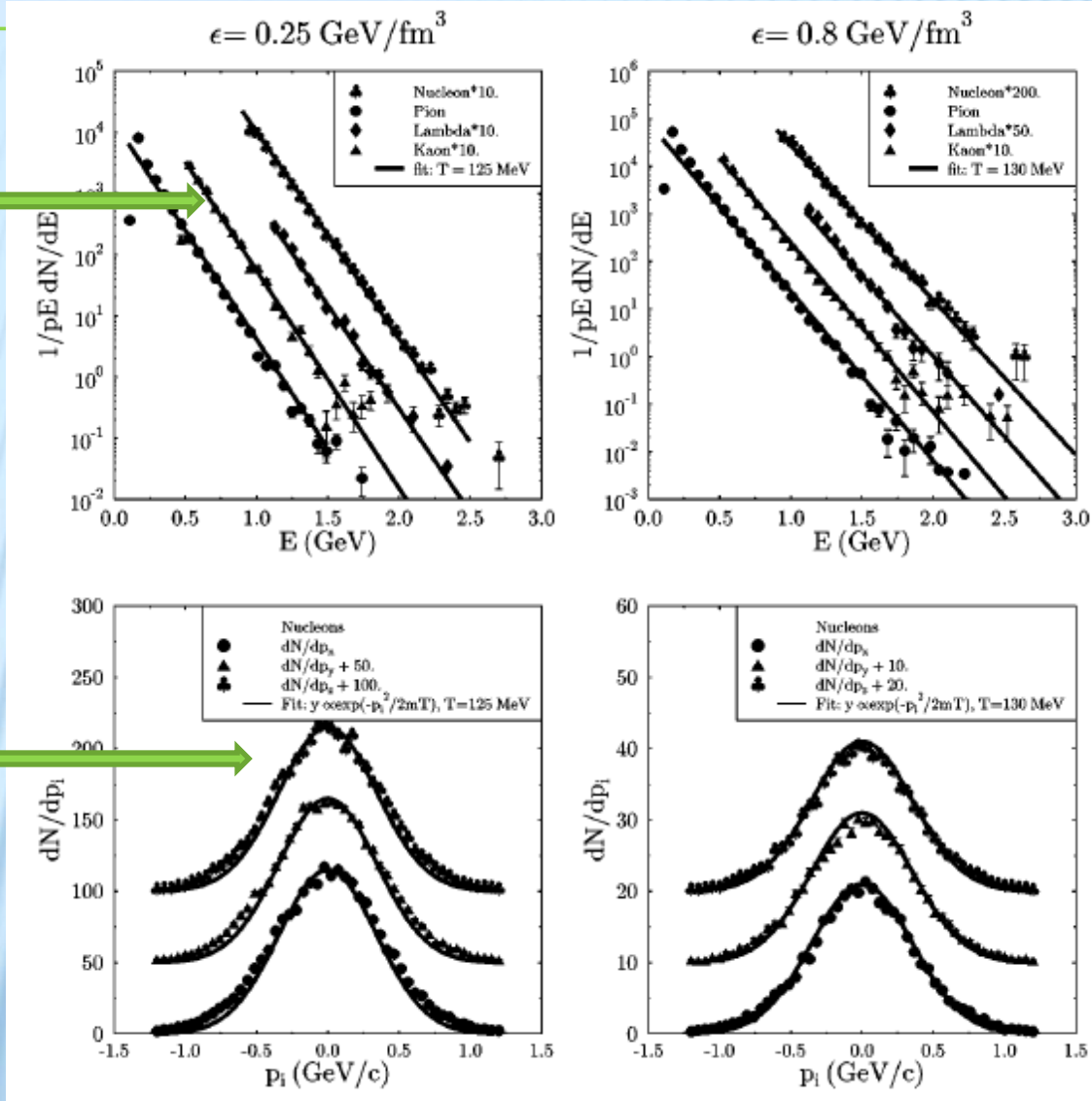


L.Bravina et al., PRC 62, 064906 (2000)

Saturation of yields after a certain time. Strange hadrons are saturated longer than others .

BOX: ENERGY SPECTRA AND MOMENTUM DISTRIBUTIONS

Fit to Boltzmann distributions $\sim \exp(-E/T)$



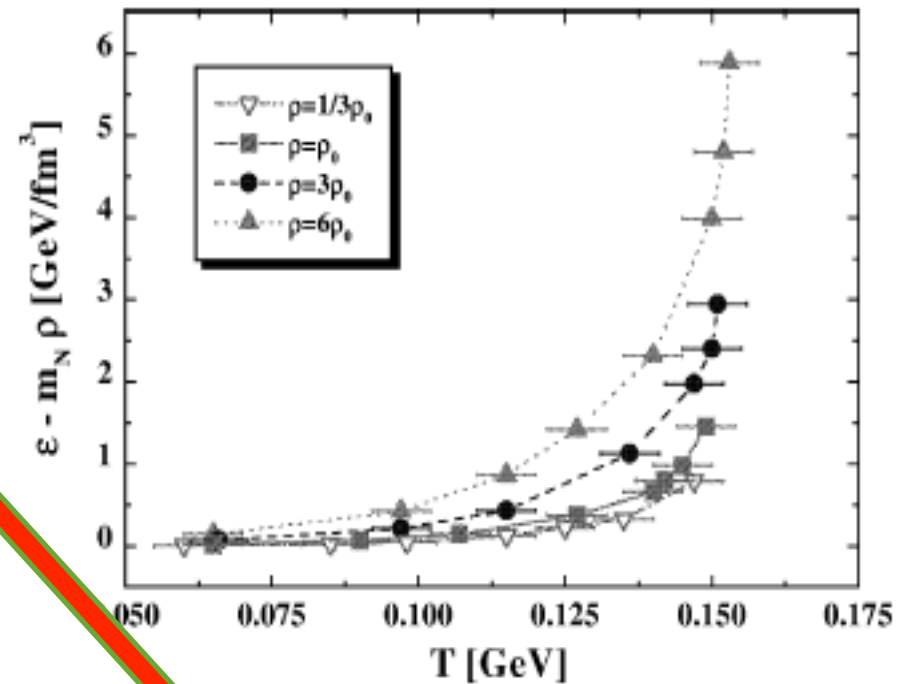
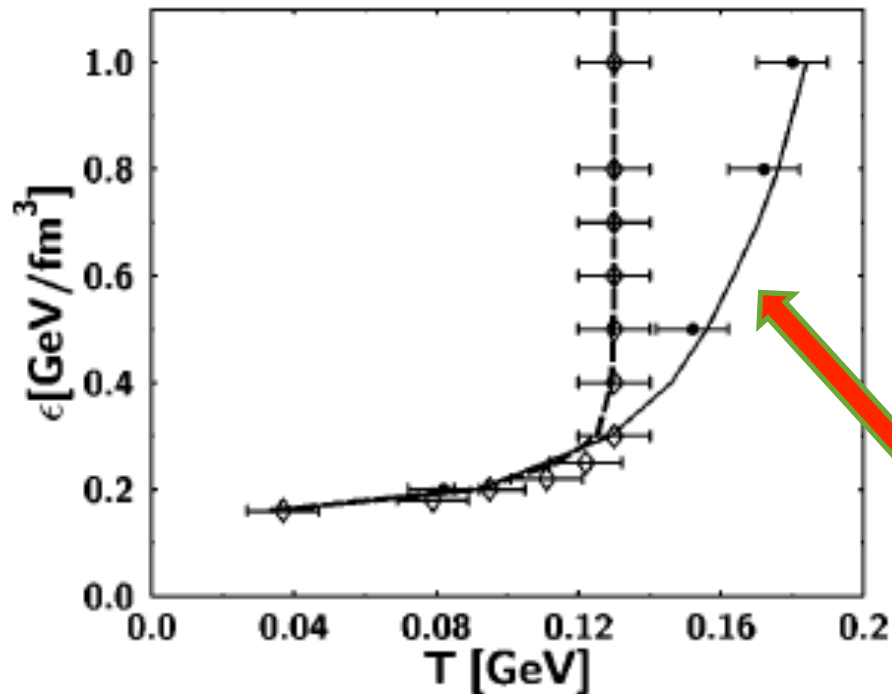
Fit to Gaussian distributions $\sim \exp(-p^2/2mT)$

Nearly the same temperature and complete isotropy of dN/dp_T

BOX: HAGEDORN-LIKE LIMITING TEMPERATURE

M.Belkacem et al., PRC 58, 1727 (1998)

HSD



UrQMD

E.Bratkovskaya et al., NPA 675, 661 (2000)

A rapid rise of T at low ϵ and saturation at high energy densities. Saturation temperature depends on number of resonances in the model. W/o strings and many-N decays – no limiting T is observed.

**Freeze-out of main
hadron species**

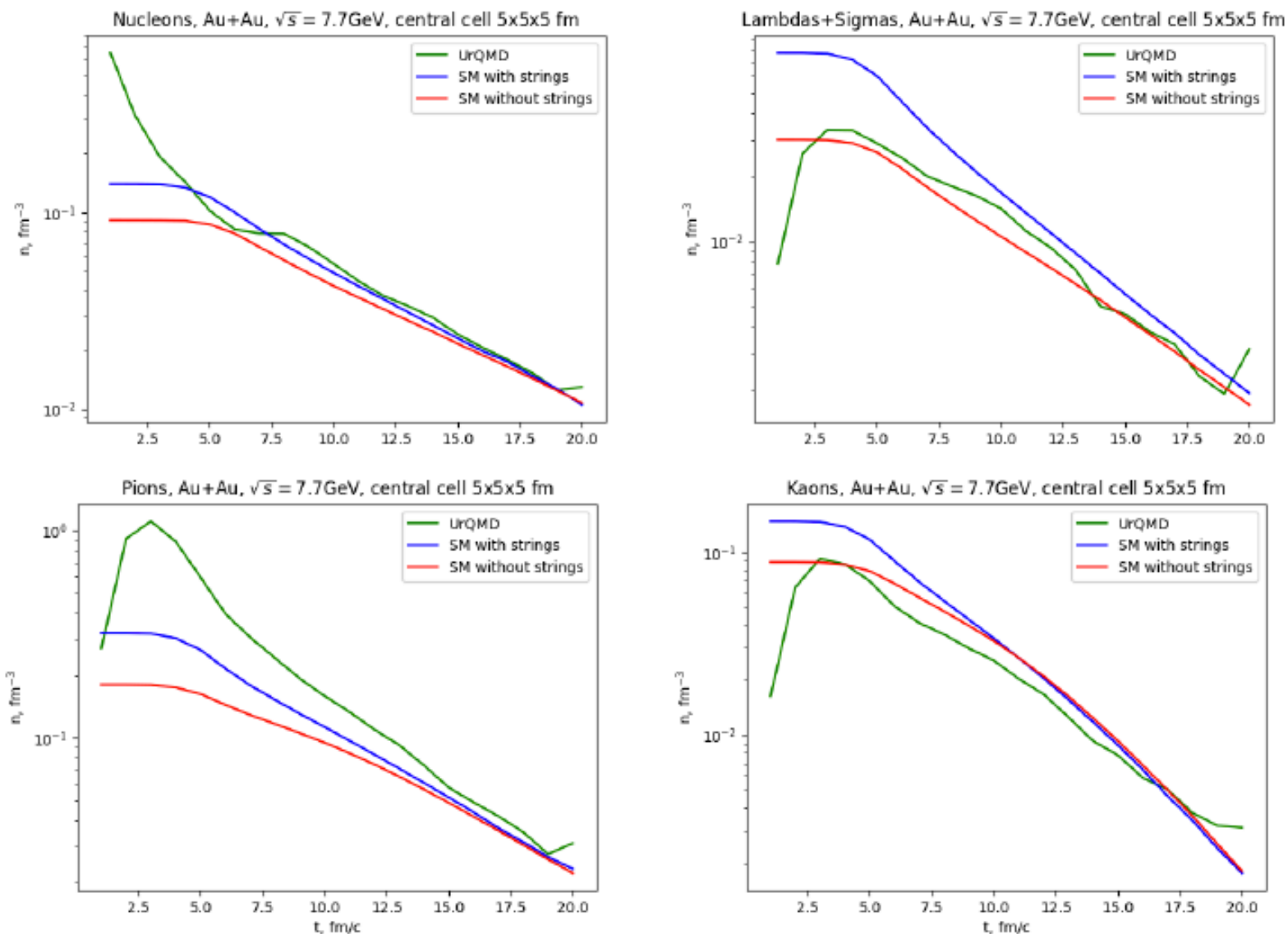


Figure 1: Particle densities in the central cell at times 1 – 20 fm/c.

Different particles
are frozen at different space
times
with different values of
 $T-\mu_B-\mu_S$

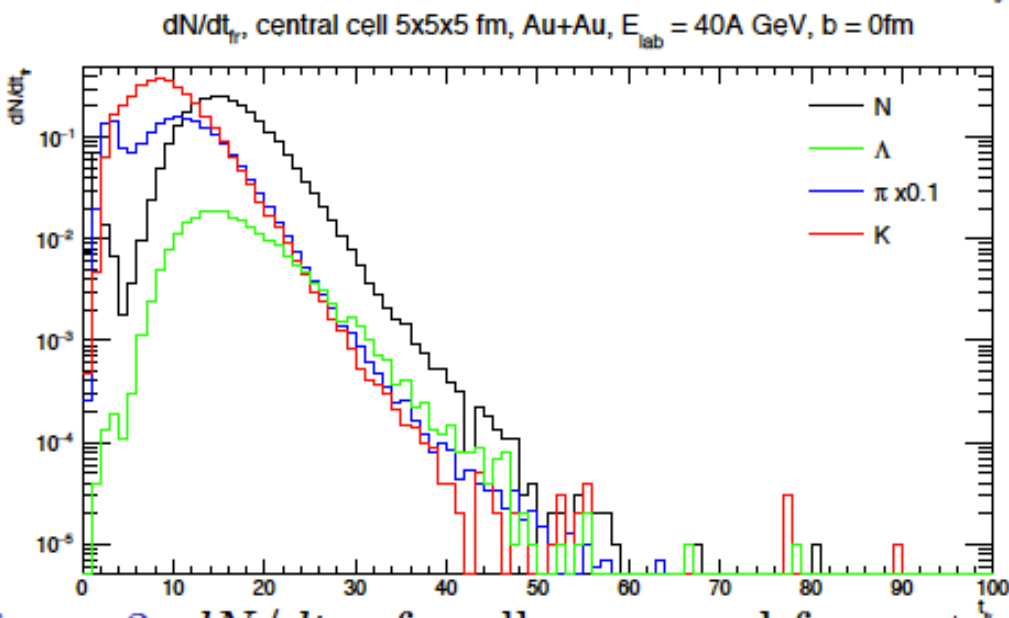
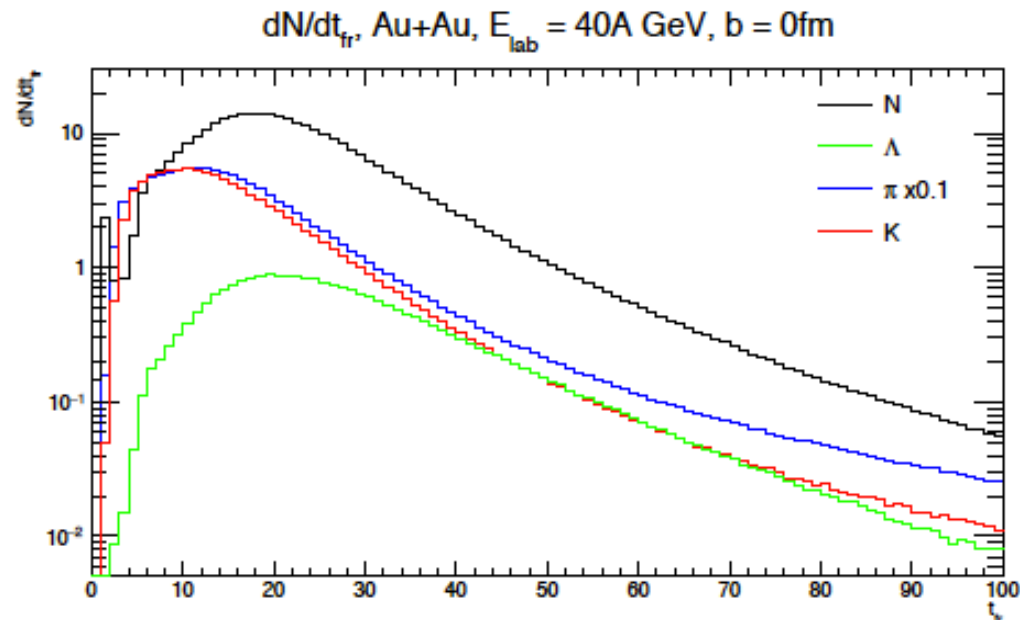


Figure 3: dN/dt_{fr} for all space and for central cell.

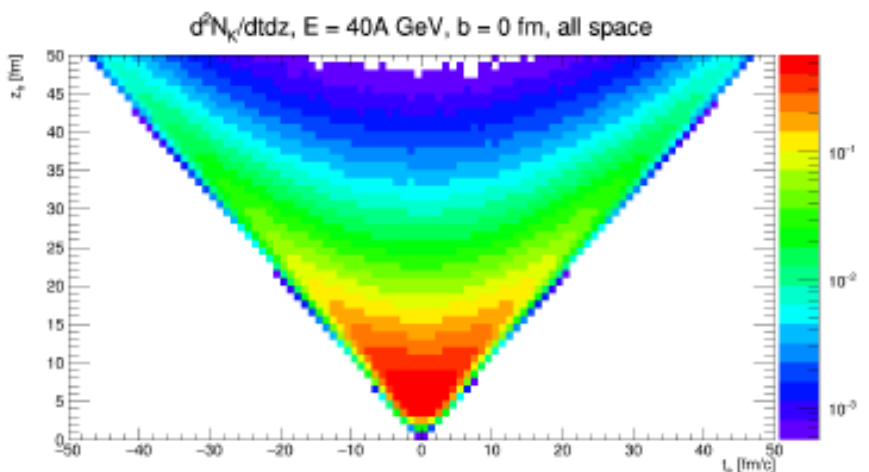
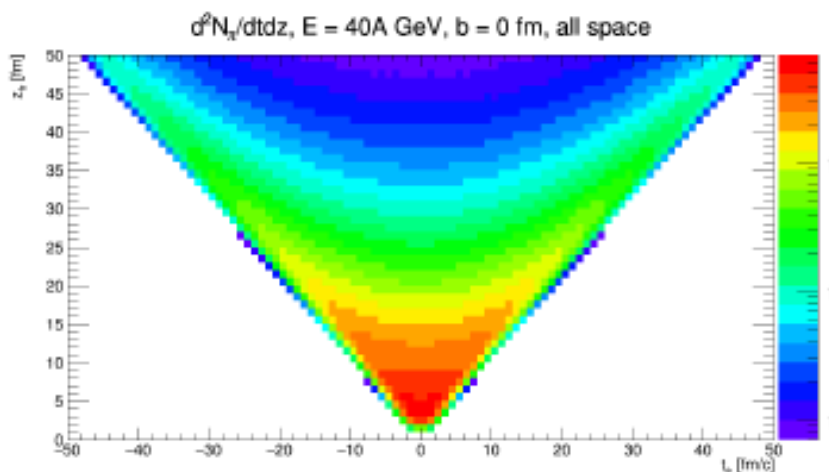
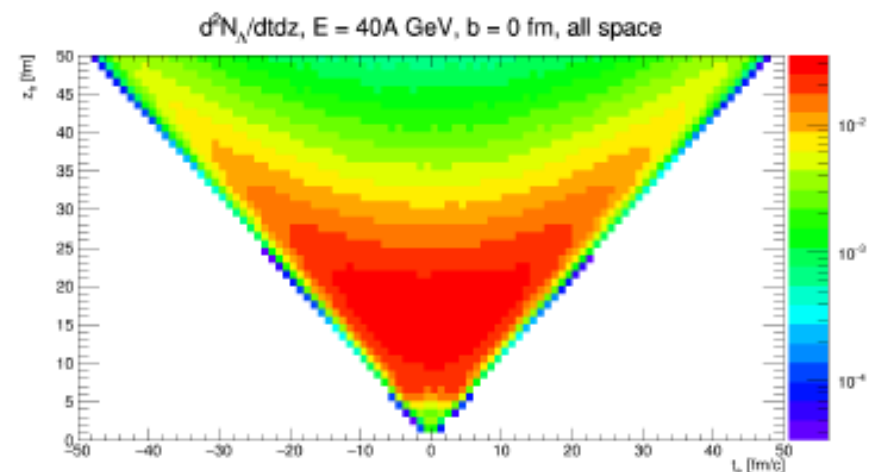
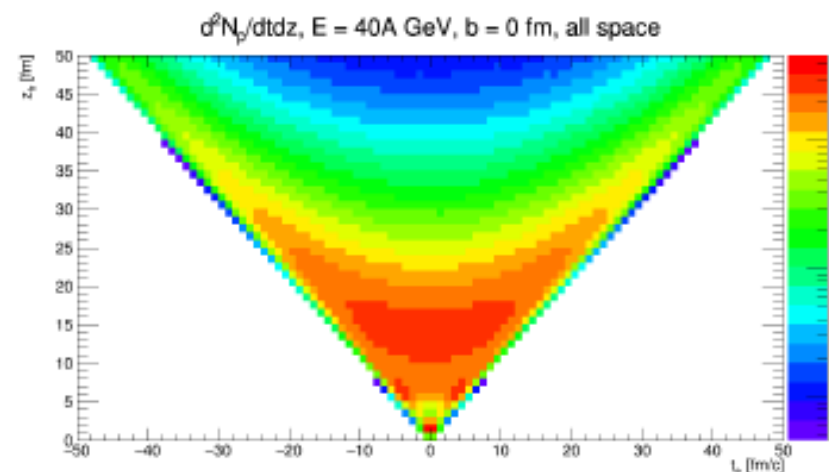


Figure 4: $d^2N/dtdz$ for protons, lambdas, pions and kaons.

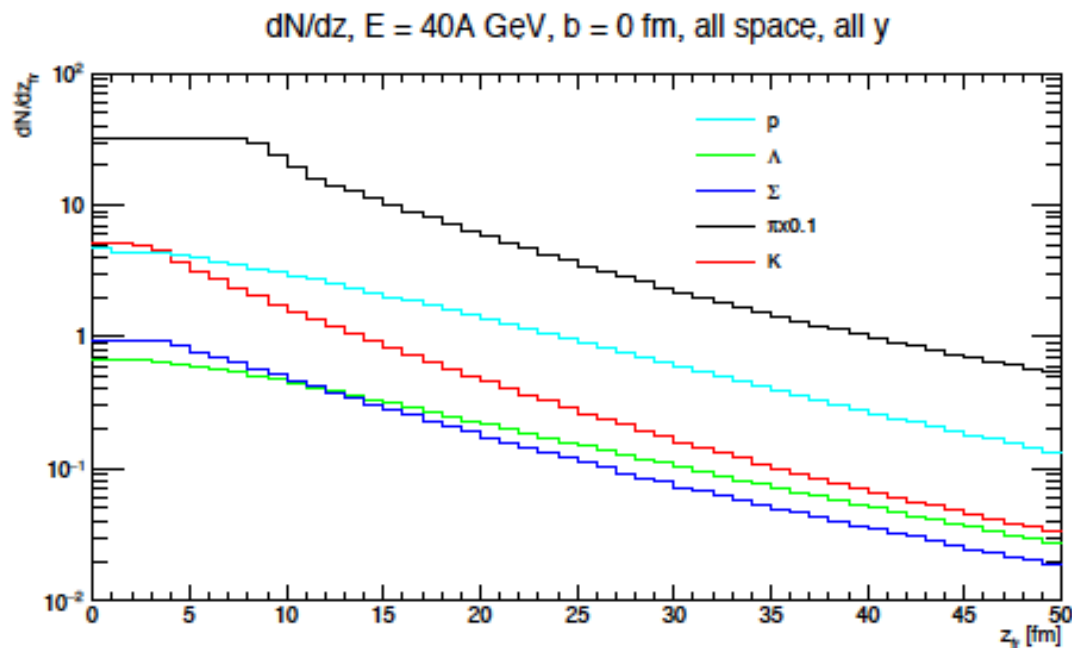


Figure 5: dN/dz for protons, lambdas, sigmas, pions and kaons for all rapidities (top figure) and for $|y| < 1$ (bottom figure). One can see that there are much more particles with large z for all rapidities, than for $|y| < 1$.

Au+Au, $E_{lab}=10A$ GeV, $b = 0$ fm, all space

	All y						$ y < 1$					
	t , fm/c	$ x , y $, fm	$ z $, fm	T , MeV	μ_b , MeV	μ_s , MeV	t , fm/c	$ x , y $, fm	$ z $, fm	T , MeV	μ_b , MeV	μ_s , MeV
All	18.0	4.7	6.4	112.4	473.1	72.1	18.1	4.9	5.3	110.6	492.3	70.8
p	19.7	4.7	7.2	108.6	478.1	63.0	19.6	4.9	5.7	101.9	524.5	72.5
\bar{p}	19.1	5.9	7.8	109.0	459.1	64.5	18.3	6.4	5.8	106.1	462.1	66.6
Λ	24.6	5.5	8.1	90.4	539.8	50.4	24.4	5.7	7.1	92.2	532.3	49.4
$\bar{\Lambda}$	23.3	6.6	8.6	98.2	487.0	58.0	22.7	6.8	7.2	96.4	497.4	54.1
Σ	20.4	4.7	6.4	105.0	496.4	56.8	20.3	4.8	5.7	101.9	524.5	72.5
$\bar{\Sigma}$	20.0	5.5	7.5	106.3	472.7	62.3	19.5	5.7	6.4	104.0	489.4	62.4
π	16.9	4.7	6.1	116.8	448.5	69.0	17.0	4.9	5.1	114.6	471.2	73.4
K	14.4	3.7	4.4	128.1	457.4	83.5	14.4	3.9	3.8	124.8	486.1	93.8
\bar{K}	20.9	5.3	7.1	102.9	486.2	59.9	20.8	5.5	6.1	101.0	500.6	64.8

Table 1: Average coordinates of freezeout and T , μ_b , μ_s at this coordinates.

Au+Au, $E_{lab}=20A$ GeV, $b = 0$ fm, all space

	All y						$ y < 1$					
	t , fm/c	$ x , y $, fm	$ z $, fm	T , MeV	μ_b , MeV	μ_s , MeV	t , fm/c	$ x , y $, fm	$ z $, fm	T , MeV	μ_b , MeV	μ_s , MeV
All	18.2	4.8	8.4	120.8	396.0	57.9	17.7	5.2	6.3	112.0	419.9	55.2
p	21.0	4.9	10.0	113.1	406.5	51.0	19.9	5.2	6.9	105.2	447.6	47.2
\bar{p}	20.0	6.4	9.5	110.3	390.0	51.1	18.2	7.0	6.4	110.2	406.8	52.9
Λ	26.0	5.9	11.2	93.9	481.9	34.0	25.0	6.1	8.6	90.7	488.4	48.5
$\bar{\Lambda}$	25.0	7.1	11.5	98.7	435.9	50.8	23.7	7.5	8.7	95.5	463.2	41.4
Σ	21.3	4.9	9.0	106.4	444.0	51.8	20.7	5.1	7.0	103.8	444.9	49.0
$\bar{\Sigma}$	21.1	6.2	9.4	107.1	409.4	45.5	20.1	6.6	7.3	106.0	429.6	43.1
π	16.9	4.8	7.8	121.6	394.8	66.1	16.6	5.1	6.0	115.6	397.7	55.0
K	15.1	4.0	6.3	131.8	374.8	68.0	14.8	4.2	4.9	120.6	416.2	59.6
\bar{K}	20.3	5.3	8.8	110.5	419.1	44.7	19.7	5.6	6.8	105.2	447.6	47.2

Table 2: Average coordinates of freezeout and T , μ_b , μ_s at this coordinates.

Au+Au, $E_{lab}=30A$ GeV, $b = 0$ fm, all space

	All y						$ y < 1$					
	t , fm/c	$ x , y $, fm	$ z $, fm	T , MeV	μ_b , MeV	μ_s , MeV	t , fm/c	$ x , y $, fm	$ z $, fm	T , MeV	μ_b , MeV	μ_s , MeV
All	18.6	5.0	9.7	120.1	370.0	42.9	17.6	5.3	6.8	113.2	393.4	47.9
p	22.3	5.1	12.0	115.5	355.4	35.5	20.3	5.4	7.5	108.8	404.4	52.3
\bar{p}	20.7	6.6	10.7	111.4	373.6	38.0	18.4	7.2	6.7	107.9	363.1	33.8
Λ	27.2	6.0	13.3	97.4	428.9	39.1	25.5	6.3	9.4	93.2	464.7	39.7
$\bar{\Lambda}$	26.1	7.3	12.9	97.9	420.0	35.7	24.1	7.8	9.1	96.9	431.4	34.6
Σ	22.3	5.1	10.7	109.4	392.4	37.1	21.2	5.3	7.7	104.0	427.5	45.3
$\bar{\Sigma}$	22.0	6.4	10.9	107.0	397.3	36.7	20.3	6.8	7.6	107.6	399.5	37.5
π	17.4	4.9	9.0	126.9	343.5	42.2	16.6	5.3	6.6	116.3	375.0	43.1
K	15.9	4.1	7.6	127.2	344.8	46.4	15.2	4.4	5.5	124.9	362.4	56.3
\bar{K}	20.5	5.3	9.8	114.4	380.6	50.1	19.3	5.6	7.2	112.1	393.3	49.7

Table 3: Average coordinates of freezeout and T , μ_b , μ_s at this coordinates.

Au+Au, $E_{lab}=40A$ GeV, $b = 0$ fm, all space

	All y						$ y < 1$					
	t , fm/c	$ x , y $, fm	$ z $, fm	T , MeV	μ_b , MeV	μ_s , MeV	t , fm/c	$ x , y $, fm	$ z $, fm	T , MeV	μ_b , MeV	μ_s , MeV
All	19.1	5.0	10.6	122.7	321.6	41.3	17.7	5.4	7.2	116.5	358.8	41.6
p	23.4	5.2	13.6	115.8	343.2	37.8	20.7	5.5	7.9	105.2	403.5	37.8
\bar{p}	21.5	6.7	11.5	114.9	340.4	32.7	18.8	7.2	7.0	109.0	351.8	33.6
Λ	28.3	6.2	14.9	96.2	423.3	20.2	25.9	6.5	10.0	91.0	459.3	33.3
$\bar{\Lambda}$	27.0	7.4	14.0	96.8	413.7	30.7	24.5	7.9	9.4	95.4	423.0	31.8
Σ	23.1	5.2	12.0	107.8	391.3	25.4	21.6	5.5	8.2	102.9	416.3	37.2
$\bar{\Sigma}$	22.7	6.4	11.8	107.8	380.0	28.7	20.7	6.9	7.9	103.6	402.3	42.6
π	17.8	5.0	9.8	125.6	323.4	39.1	16.7	5.4	6.9	117.5	359.8	40.5
K	16.6	4.3	8.6	126.3	332.3	42.1	15.5	4.5	5.9	120.2	371.5	52.8
\bar{K}	20.7	5.4	10.6	113.6	359.6	30.6	19.3	5.7	7.5	111.9	379.5	34.9

Table 4: Average coordinates of freezeout and T , μ_b , μ_s at this coordinates.

Consequences of the different space-time freeze-out:

- Differences in yields in SM**

The difference between average freeze-out and freeze-out for particular species is very large

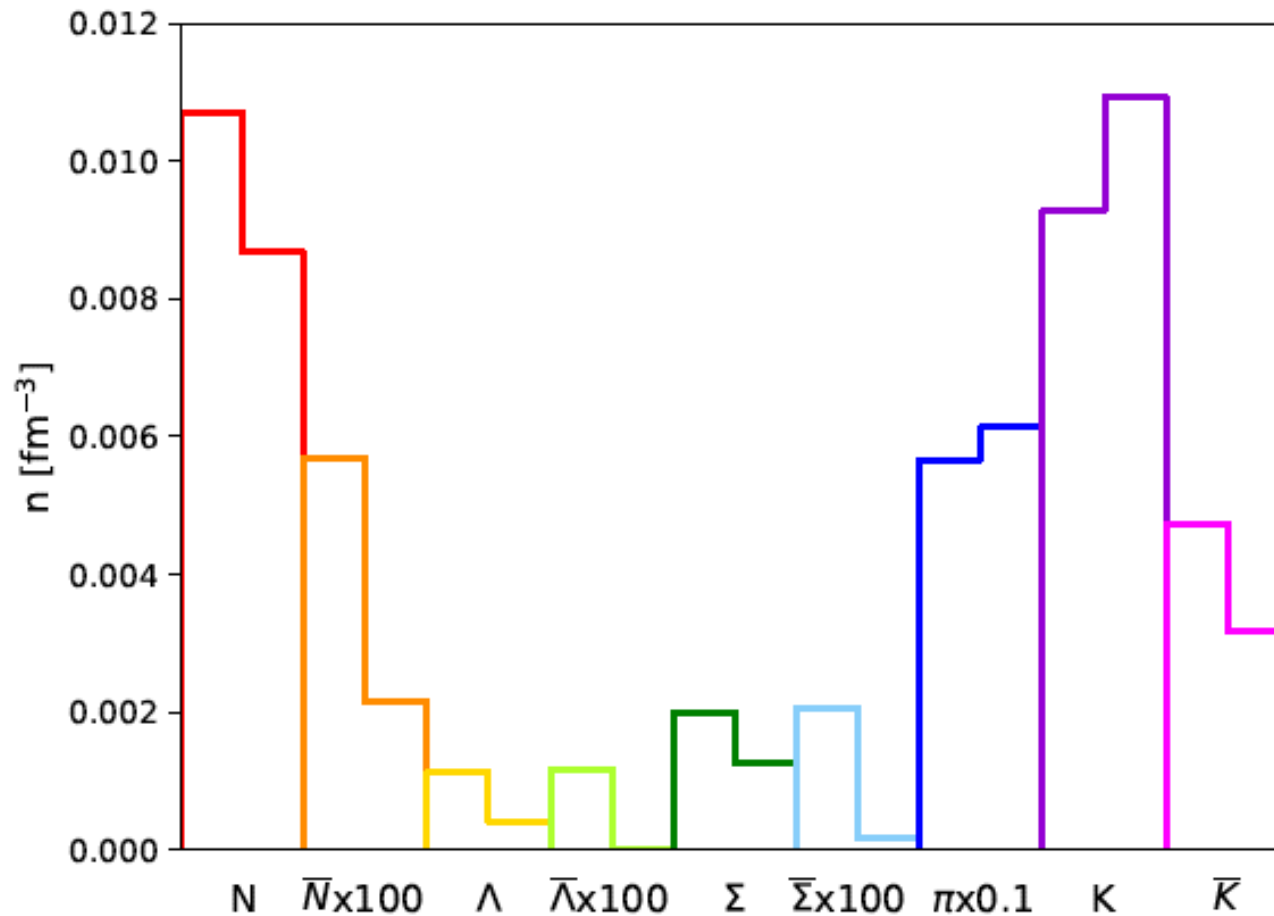


Figure 4: Particle densities at average freezeout coordinates of all particles (left column) and at freezeout coordinates of each particle type (right column) from statmodel; at average freezeout coordinates of all particles (star) and at freezeout coordinates of each particle type (pentagon) from UrQMD. $E = 40A$ GeV.

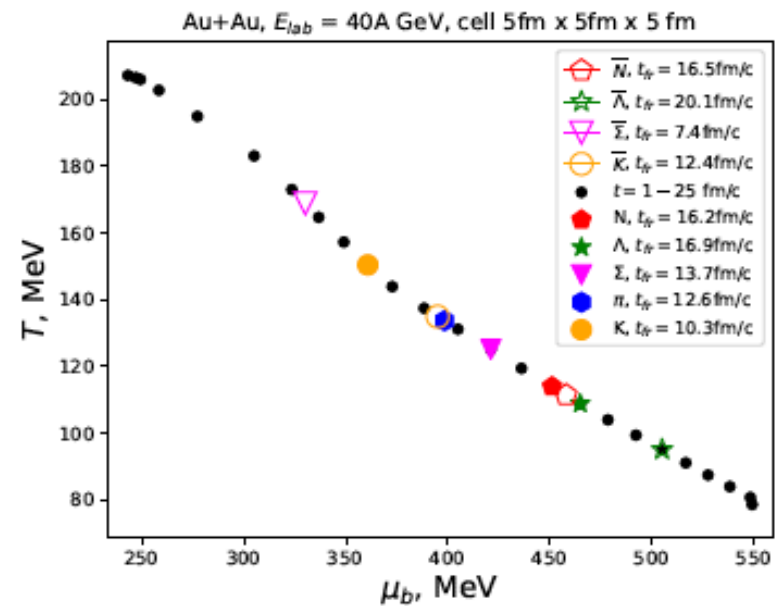
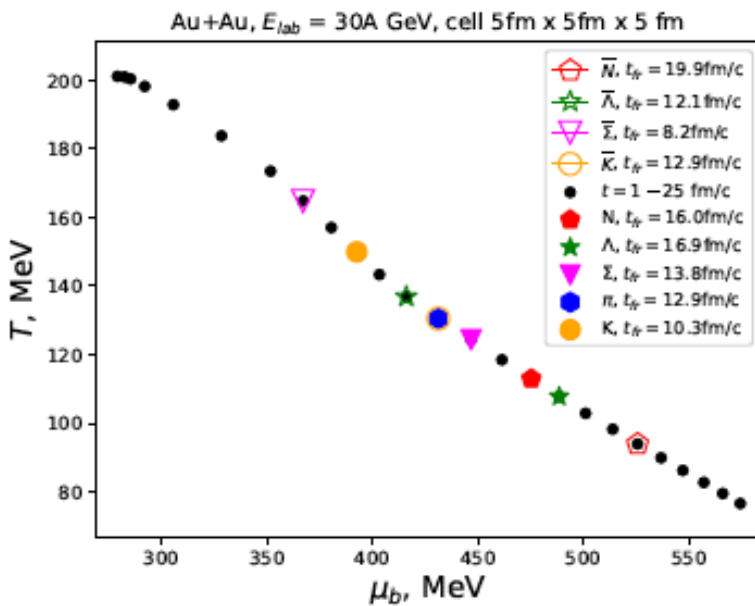
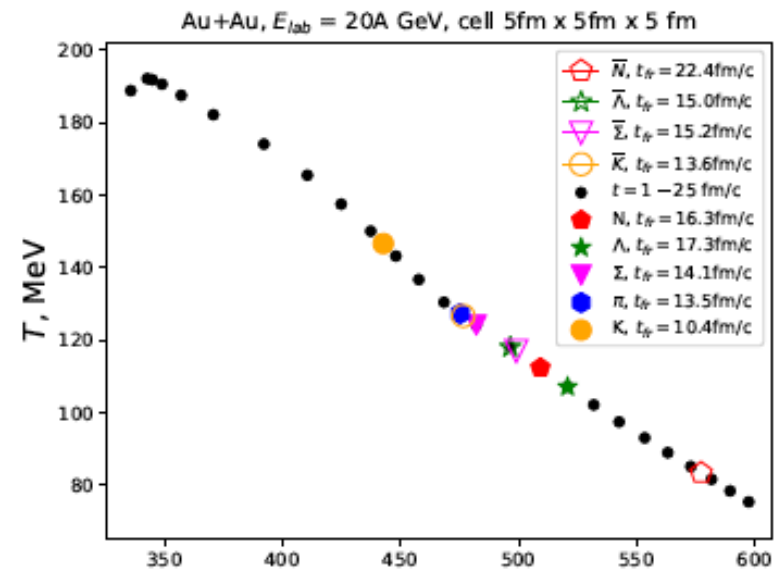
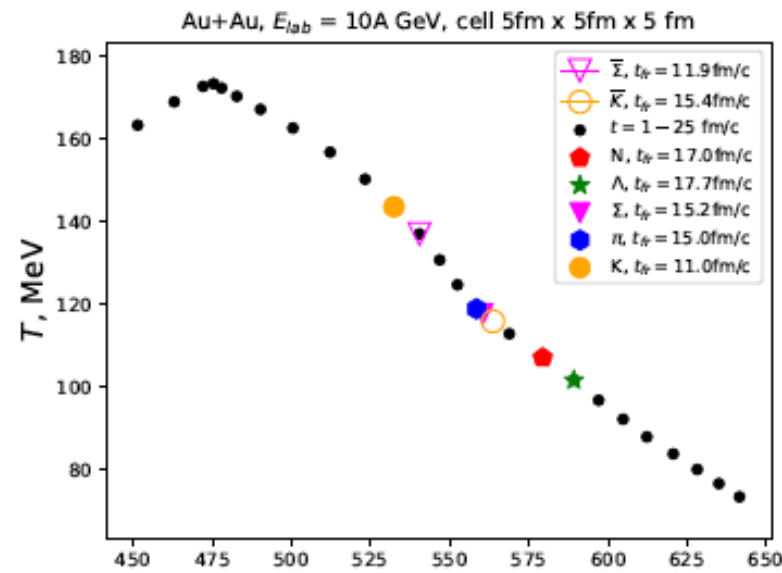


Figure 2: $T(\mu_B)$ in the central cell. Average freezeout times of different particles in the central cell are marked by colored markers.

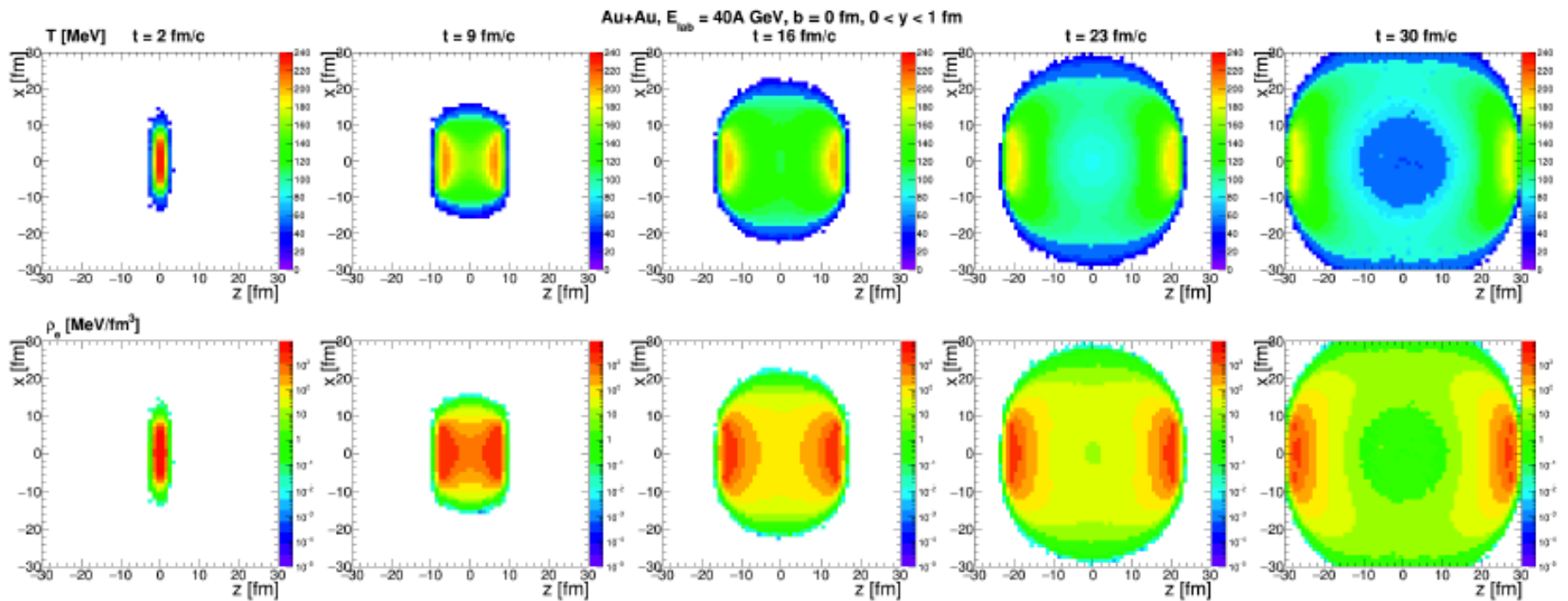


Figure 5: T and ϵ spatial distributions.

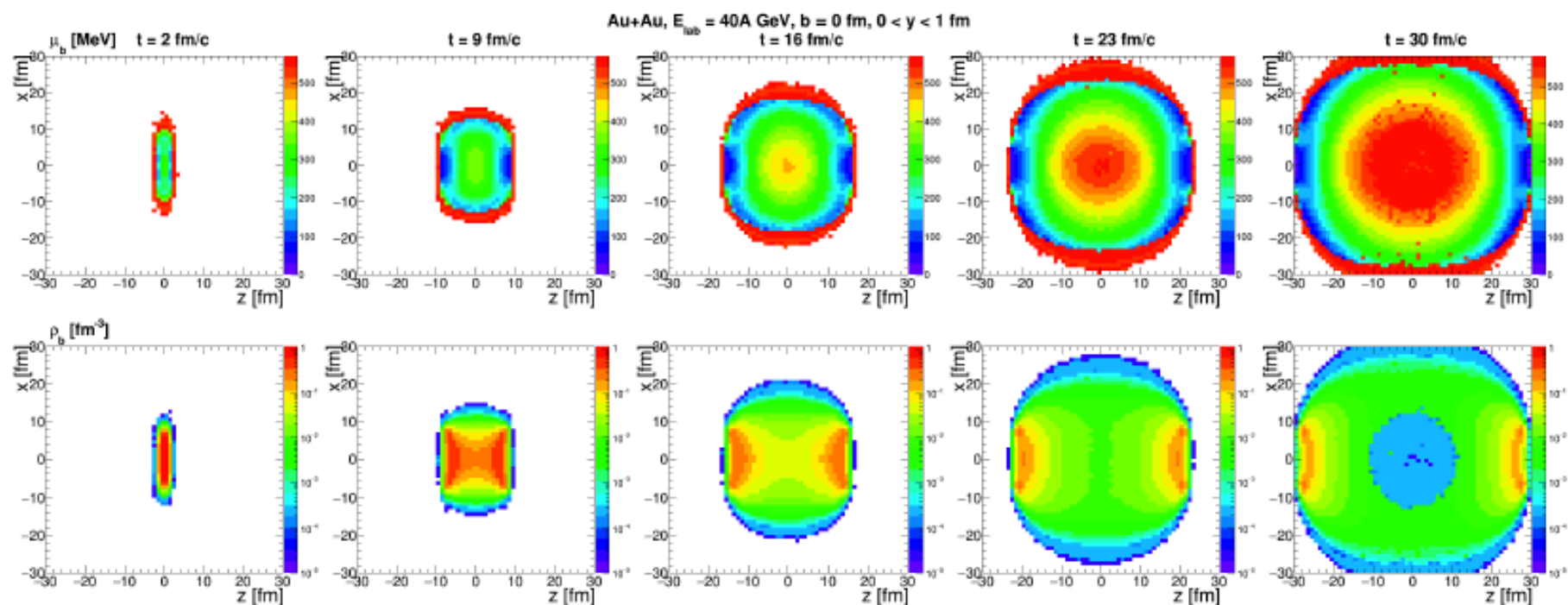


Figure 6: μ_b and ρ_b spatial distributions.

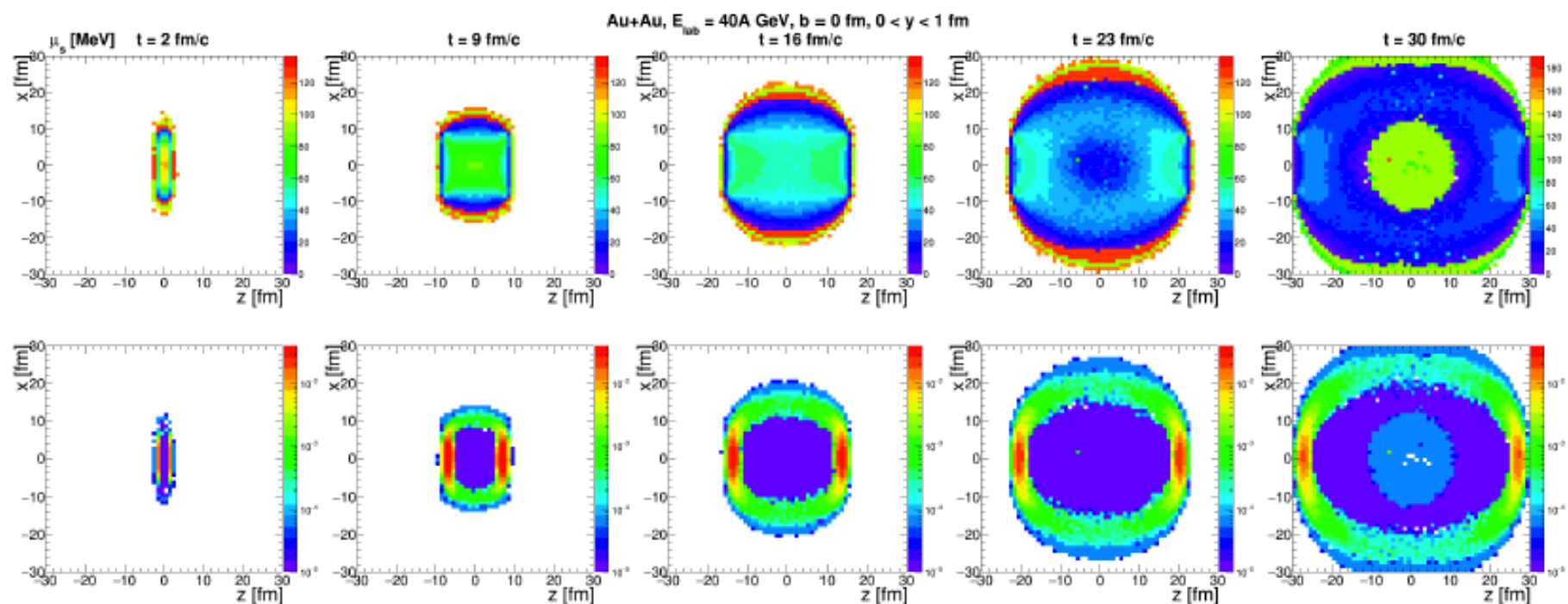
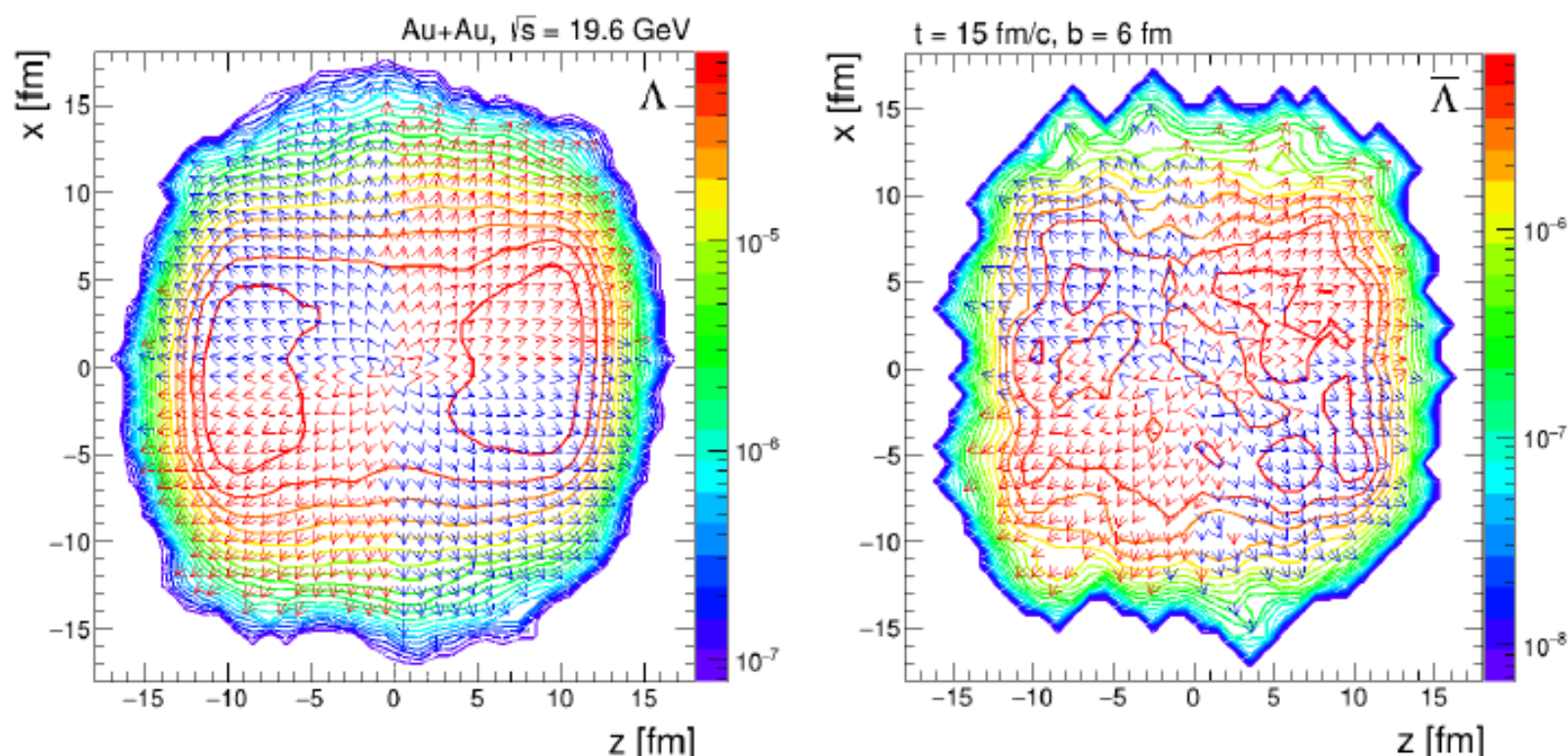


Figure 7: μ_s and ρ_s spatial distributions.

Consequences of the different space-time freeze-out:

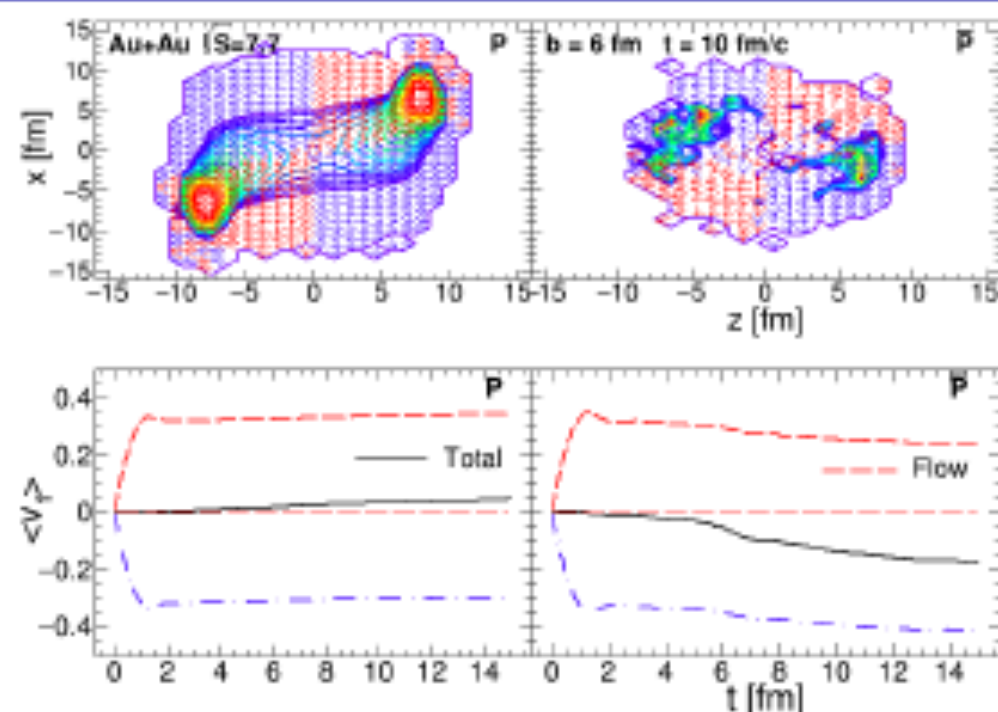
- Directed flow**

Space distribution of Lambdas



At $\sqrt{s} = 19.6$ GeV Λ are mostly located near hot and dense regions and $\bar{\Lambda}$ are distributed more uniformly near system center.

Space distribution of Lambdas



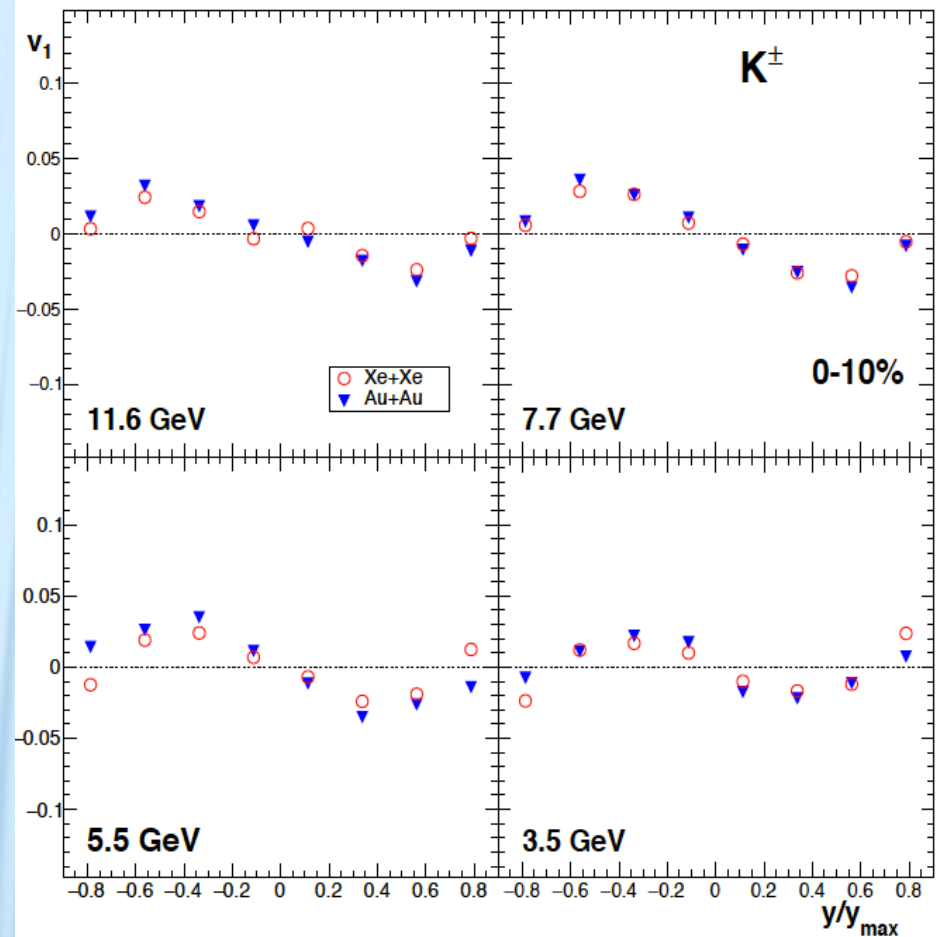
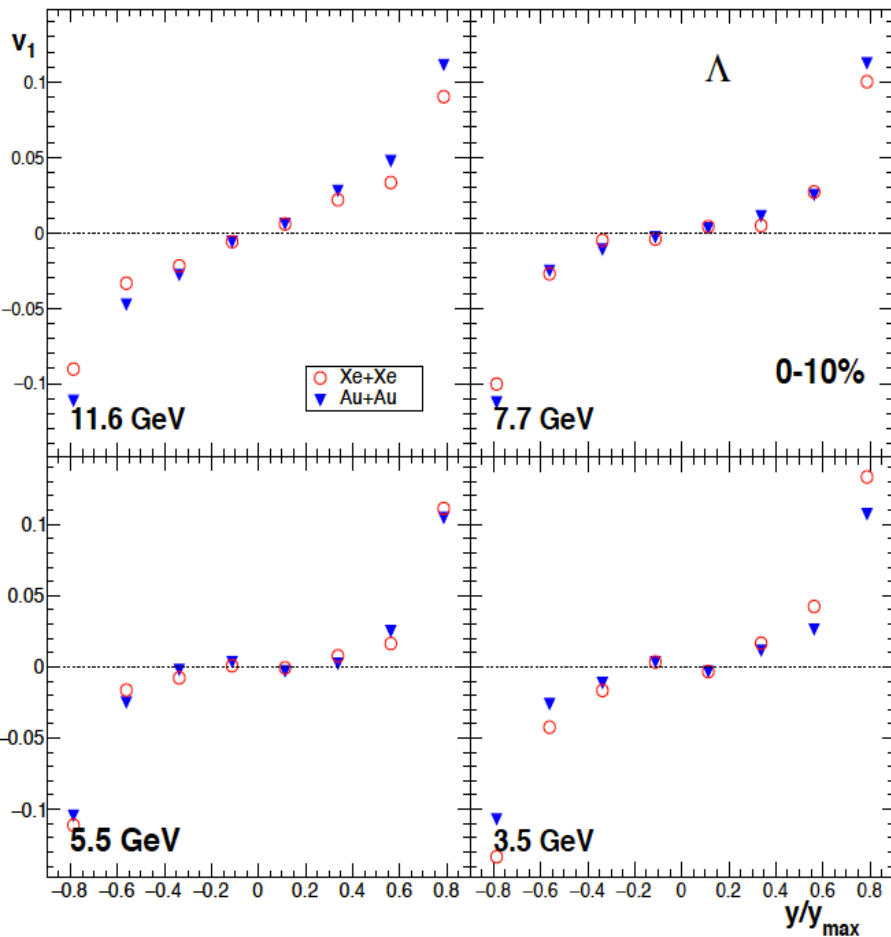
At low energies Λ and $\bar{\Lambda}$ are produced and emitted from the same regions as protons and antiprotons respectively. Λ 's are concentrated also near hot and dense spectators, whereas $\bar{\Lambda}$'s are mostly produced in central region.

Mean flow is calculated as:

$$\langle v_1 \rangle = \int \text{sign}(y) v_1(y) \frac{dN^{\text{par}}}{dy} dy / \int \frac{dN^{\text{par}}}{dy} dy$$

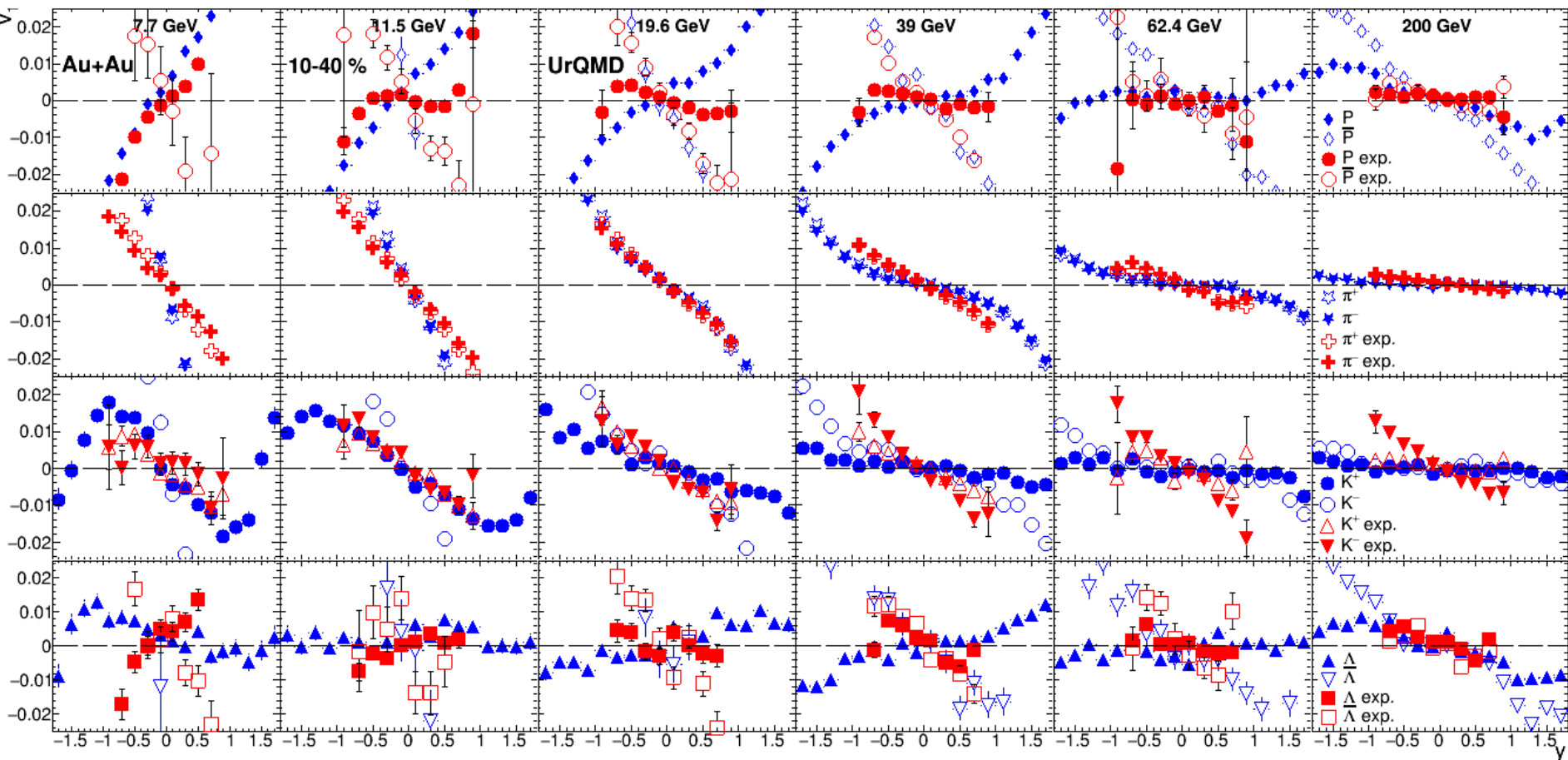
Collective velocities are shown on the picture to demonstrate that particles which have positive product of velocities $v_x v_z$ produce normal component of flow and particles with $v_x v_z < 0$ produce anti-flow component of directed flow. [Bravina et al, EPJ Web of Conferences 191, 05004 (2018)]

Directed flow for Lambdas and kaons



V_1 for Λ changes sign at midrapidity with decreasing collision energy, whereas V_1 for kaons has negative slope (antiflow)

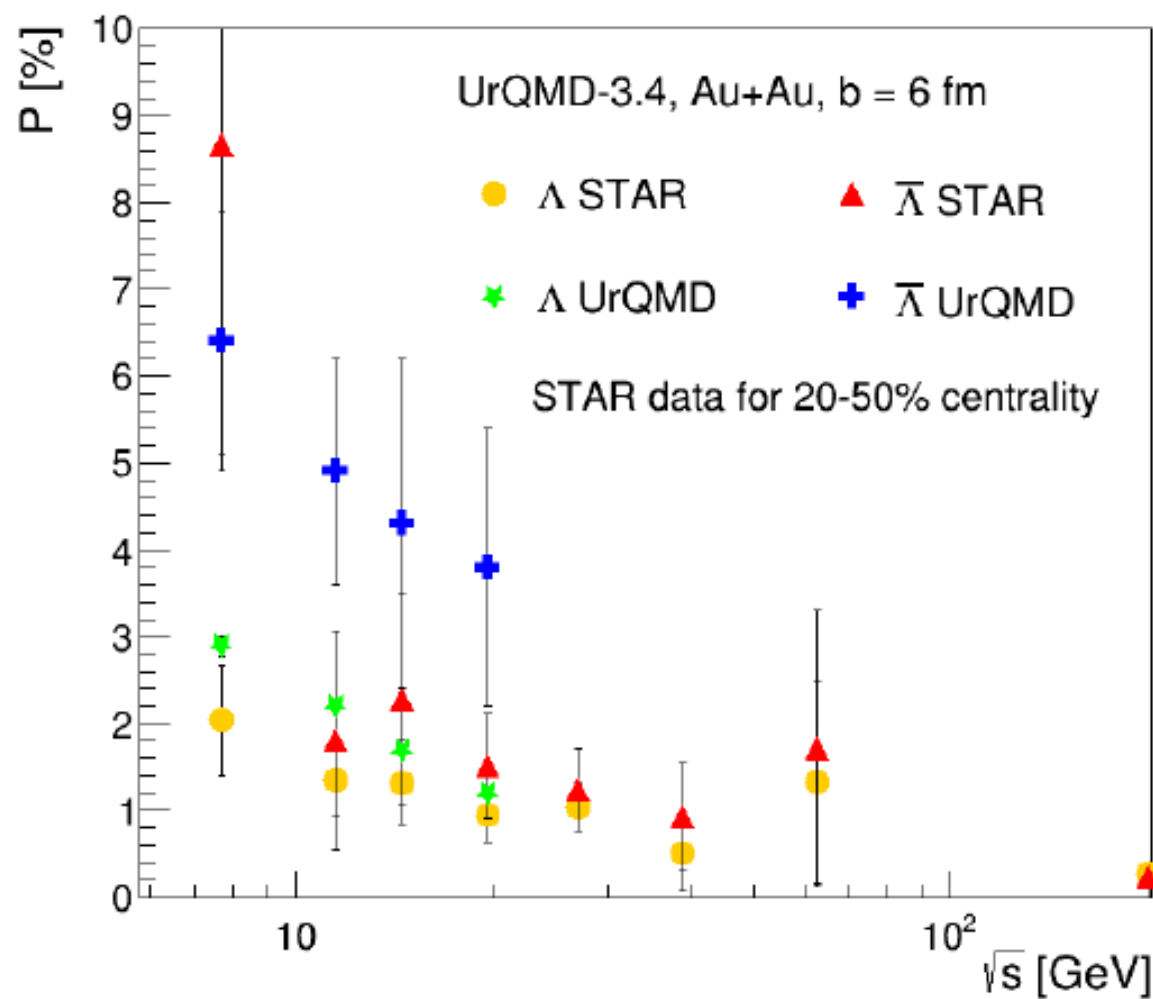
Different slopes of different particles: URQMD and Data



**Consequences of the different
space-time freeze-out:**

- Difference in Polarization
for lambdas and antilambdas**

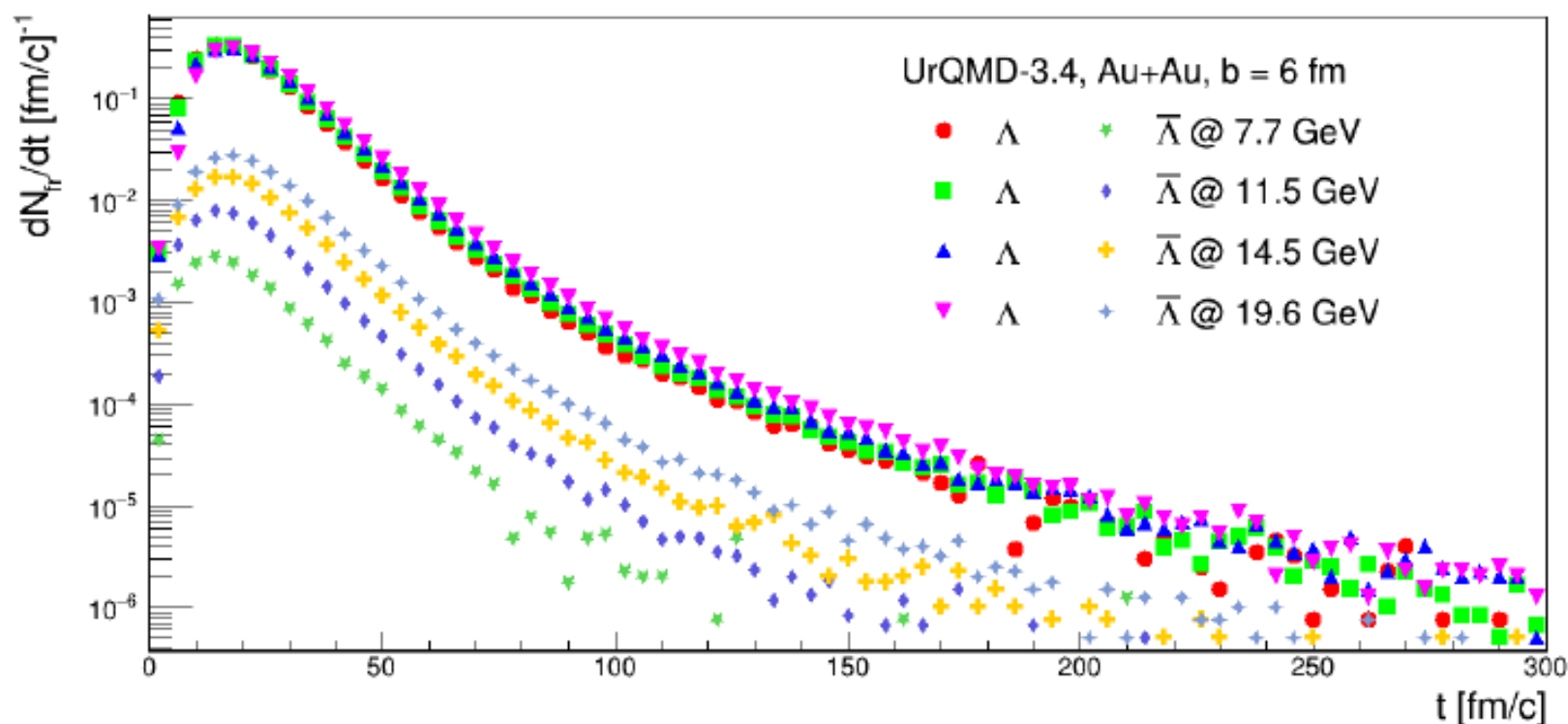
Polarization energy dependency



Polarization of Λ and $\bar{\Lambda}$ decreases with energy as in the experiment. Λ 's global polarization agrees well with experimental data. $\bar{\Lambda}$ polarization has right energy dependence.

STAR data from [Phys. Rev. C 98 (2018) 14910]

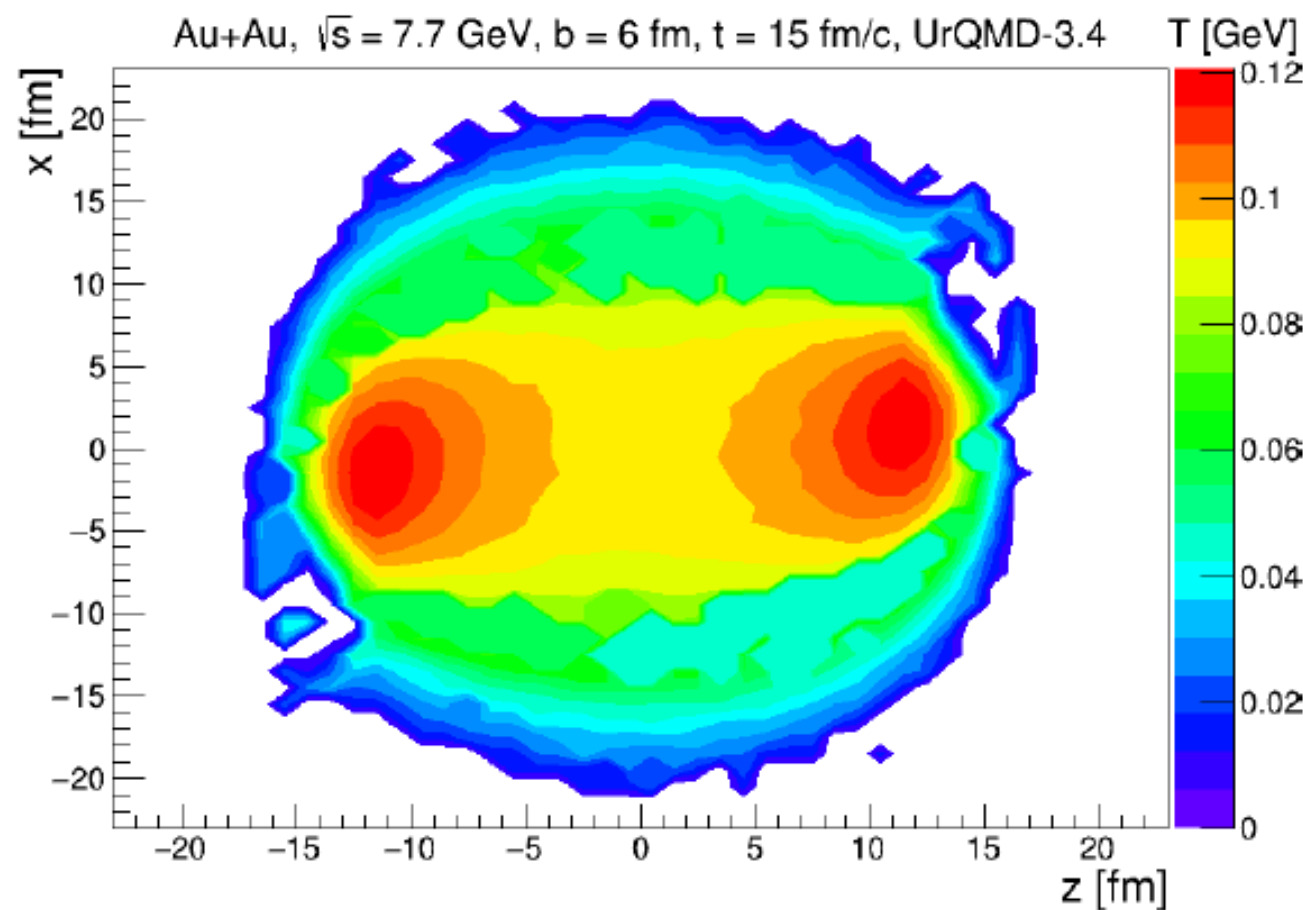
Freeze-out



Λ 's and $\bar{\Lambda}$'s with $|y| < 1$ and $0.2 < p_t < 3$ GeV/c were analyzed.

\sqrt{s} [GeV]	7.7	11.5	14.5	19.6
Mean freeze-out time Λ [fm/c]	21.3009	21.9568	23.066	24.3462
Mean freeze-out time $\bar{\Lambda}$ [fm/c]	19.7806	21.0302	21.959	23.1288

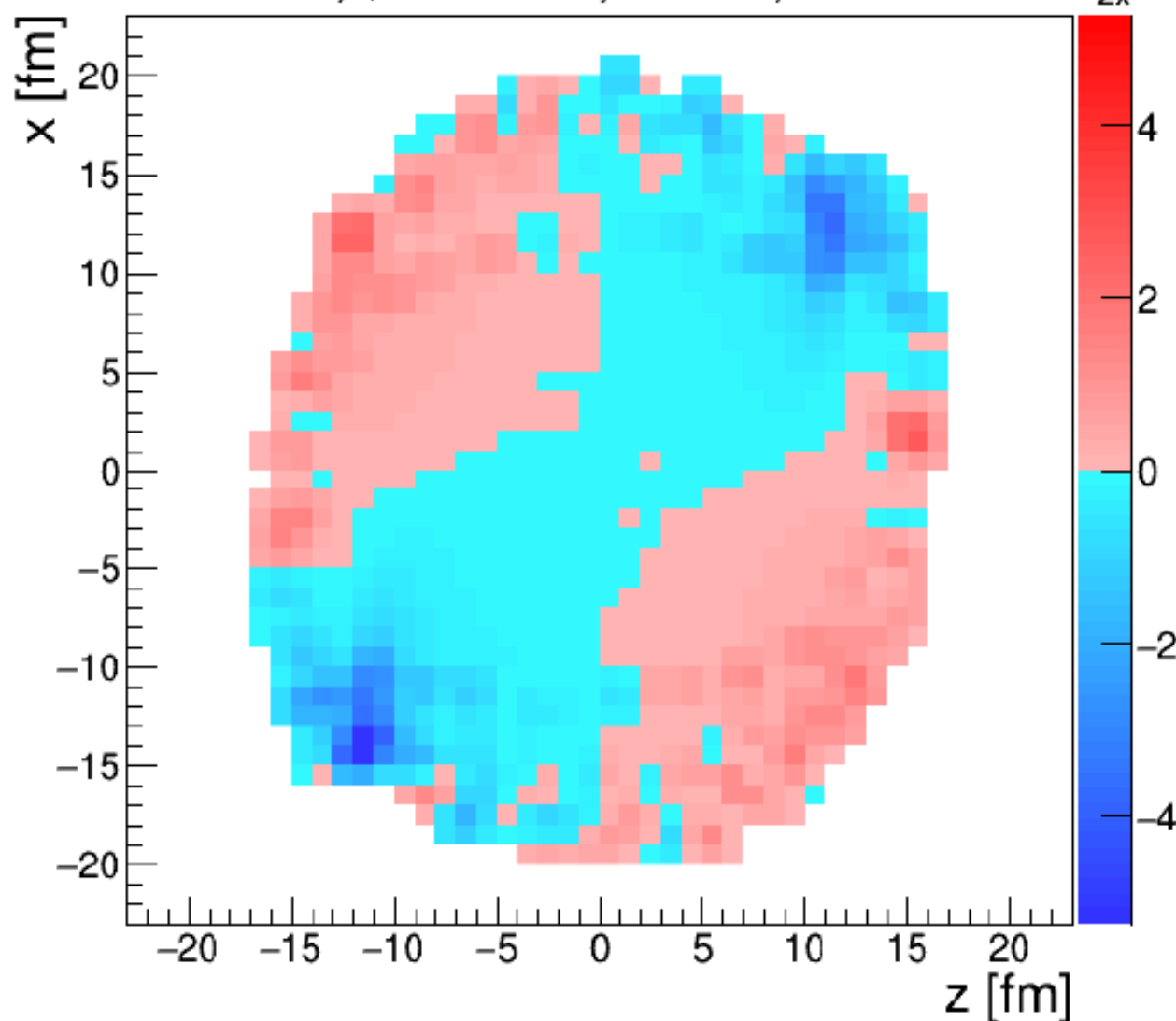
Proper Temperature



Temperature extracted with statistical model is not uniform. There are two main regions. More hot regions with $T \simeq 100 \text{ MeV}$ are connected to dense spectators. The other part is related to fireball with temperature $\simeq 60 \text{ MeV}$.

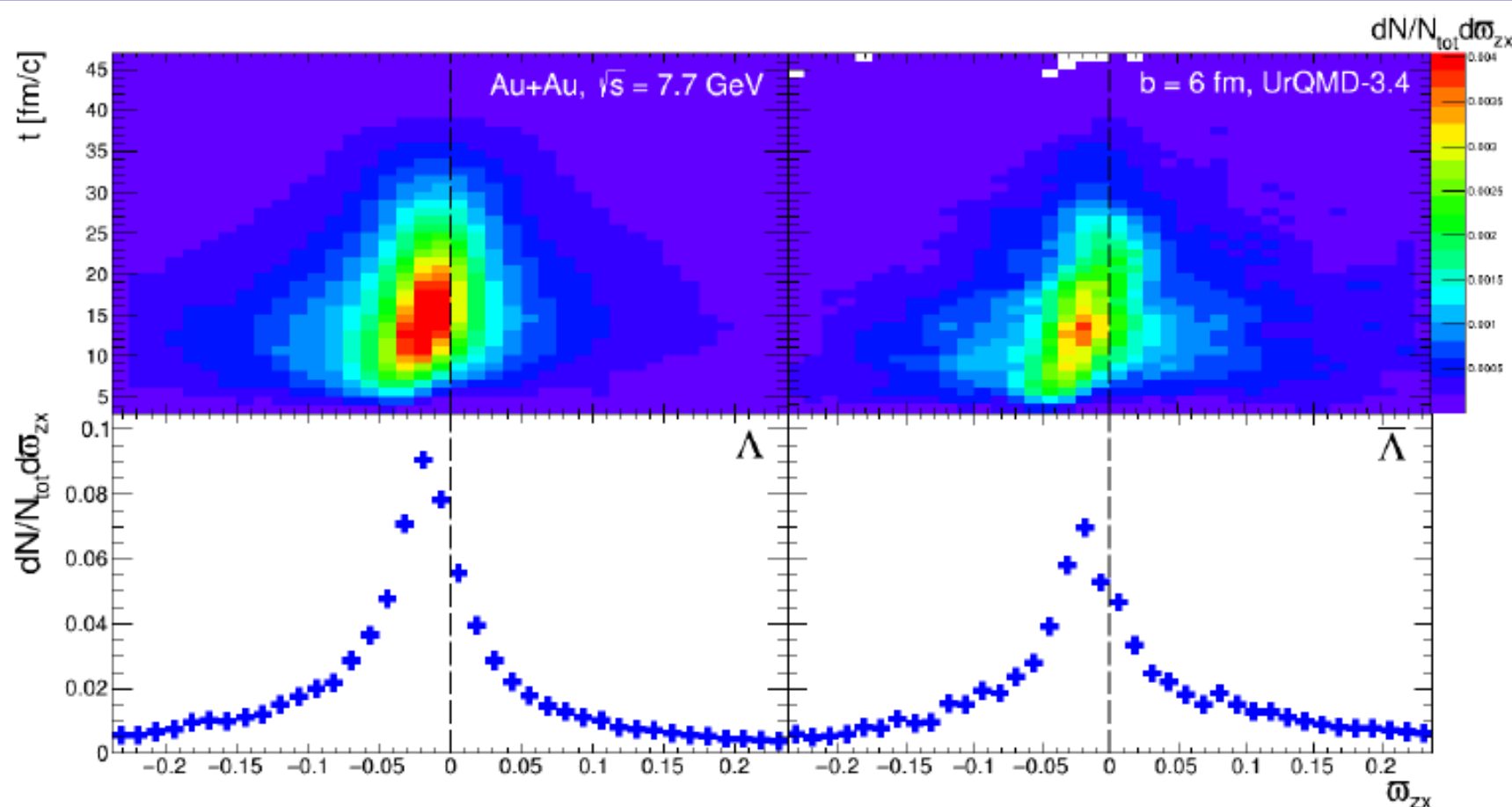
Thermal vorticity in reaction plane

Au+Au, $\sqrt{s} = 7.7$ GeV, $b = 6$ fm, $t = 15$ fm/c



Thermal vorticity component ϖ_{zx} has quadrupole-like structure in reaction plane which is stable in time but magnitude decreases due to system expansion. First and third quadrant are connected with central region which has small negative vorticity. This connection part becomes smaller when energy increases.

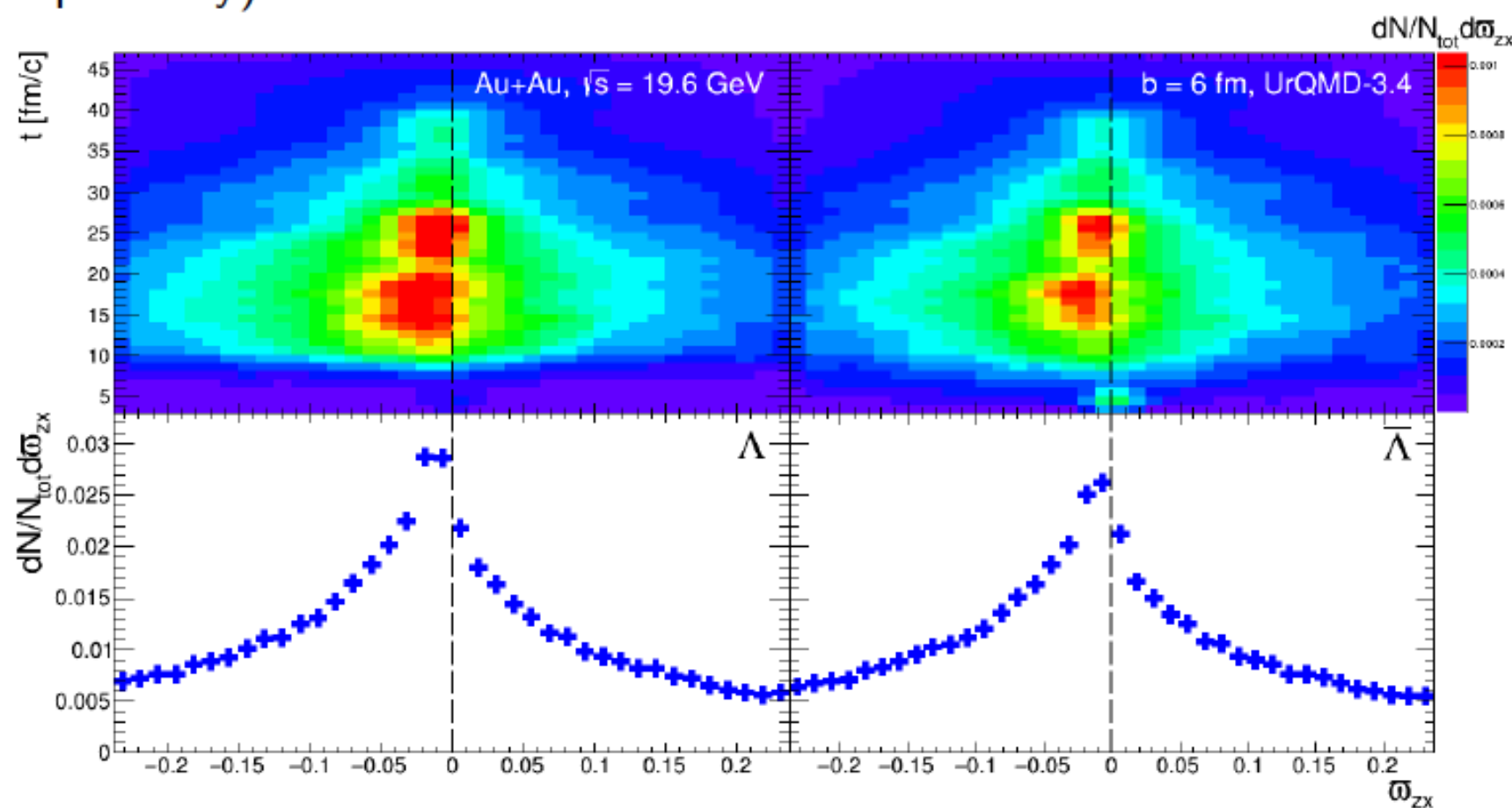
Emission of Λ and $\bar{\Lambda}$



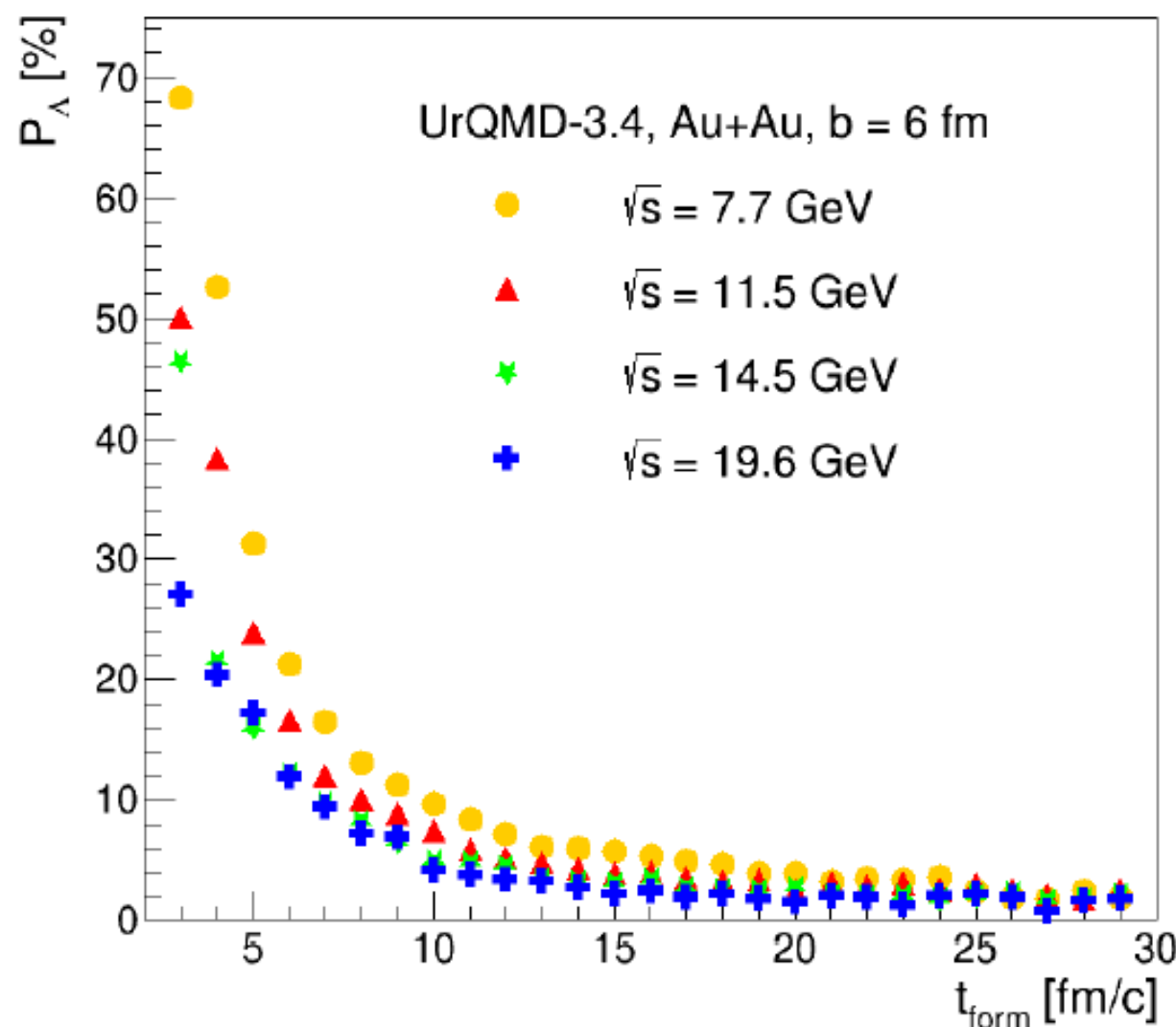
At $\sqrt{s} = 7.7 \text{ GeV}$ Λ and $\bar{\Lambda}$ are mainly emitted from regions with small negative vorticity, thus they should have non-zero positive polarization. $\bar{\Lambda}$ has mean value of ϖ_{zx} with larger magnitude than Λ ($\simeq -0.04$ and $\simeq -0.017$ respectively).

Emission of Λ and $\bar{\Lambda}$

At $\sqrt{s} = 19.6 \text{ GeV}$ Λ and $\bar{\Lambda}$ are also mainly emitted from regions with small negative vorticity, but distributions are more symmetric and wide. Thus mean values of ϖ_{zx} for Λ and $\bar{\Lambda}$ drop ($\simeq -0.009$ and $\simeq -0.011$ respectively).



Polarization time evolution



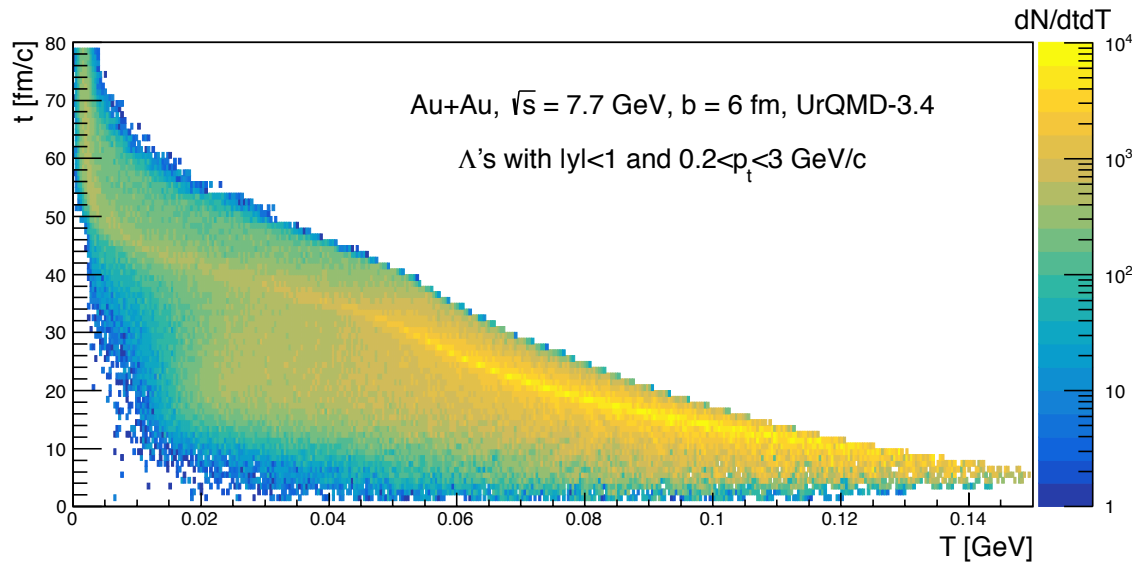
Polarization of Λ hyperon decreases with time. At the beginning lambdas are preferably formed in hot and dense regions with high polarization. But later lambdas are formed uniformly in fireball and average polarization is almost zero.

Conclusions

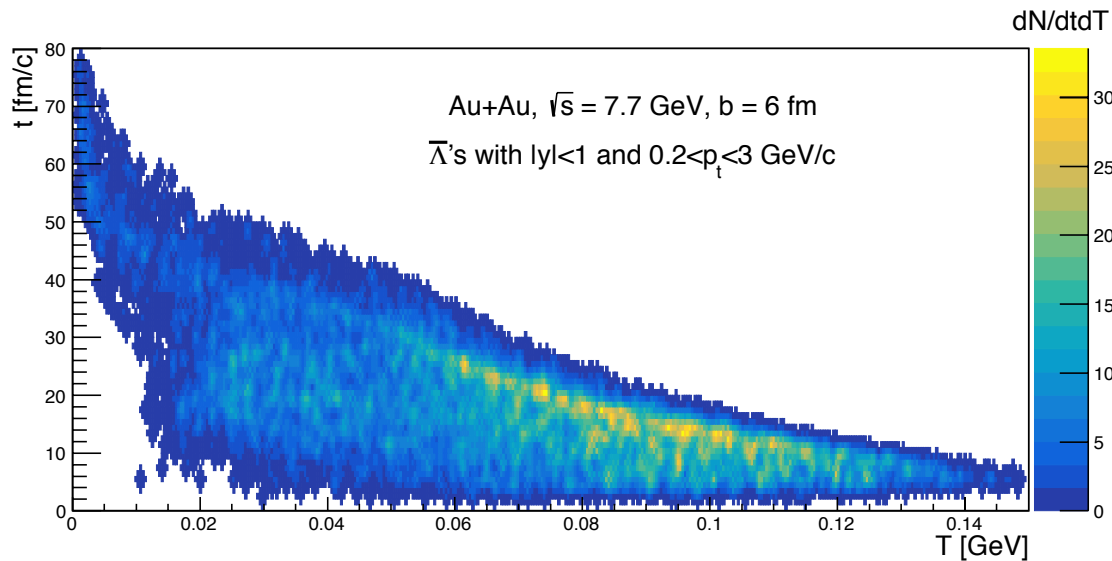
- *MC models favor chemical equilibration of hot and dense nuclear matter at $t \approx 7 \text{ fm}/c$*
- *The **EOS** has a simple form: $P/\varepsilon = \text{const}$ (hydro!) even at far-from-equilibrium stage. The speed of sound C_s^2 varies from 0.12 (AGS) to 0.14 (40 AGeV), and to 0.15 (SPS & RHIC) => saturation*
- *In MC models different particles are frozen at different times: K - π -anti Σ - Σ , anti p - p -anti Λ - Λ and in different space regions with different T - μ_B - μ_S*
It naturally explains such effects as directed flow for p , Σ , Λ and antiflow for K -anti Σ -, anti p -anti Λ , higher polarization for anti- Λ than for Λ

Back-up Slides

Single-particle method for extraction $T-\mu_B-\mu_S$



gives more precise
estimation of
average $T-\mu_B-\mu_S$



Thermal Approach

In local thermal equilibrium, the ensemble average of the spin vector for spin-1/2 fermions with four-momentum p at space-time point x is obtained from the statistical-hydrodynamical model as well as the Wigner function approach and reads

$$S^\mu(x, p) = -\frac{1}{8m} (1 - n_F) \epsilon^{\mu\nu\rho\sigma} p_\nu \varpi_{\rho\sigma}(x),$$

where the thermal vorticity tensor is given by

$$\varpi_{\mu\nu} = \frac{1}{2} (\partial_\nu \beta_\mu - \partial_\mu \beta_\nu),$$

with $\beta^\mu = u^\mu / T$ being the inverse-temperature four-velocity. The number density of Λ 's is very small so that we can make the approximation $1 - n_F \simeq 1$ Therefore:

$$S^\mu(x, p) = -\frac{1}{8m} \epsilon^{\mu\nu\rho\sigma} p_\nu \varpi_{\rho\sigma}(x).$$

By decomposing the thermal vorticity into the following components,

$$\varpi_T = (\varpi_{0x}, \varpi_{0y}, \varpi_{0z}) = \frac{1}{2} \left[\nabla \left(\frac{\gamma}{T} \right) + \partial_t \left(\frac{\gamma \mathbf{v}}{T} \right) \right],$$

$$\varpi_S = (\varpi_{yz}, \varpi_{zx}, \varpi_{xy}) = \frac{1}{2} \nabla \times \left(\frac{\gamma \mathbf{v}}{T} \right),$$

Equation can be rewritten as

$$S^0(x, p) = \frac{1}{4m} \mathbf{p} \cdot \varpi_S, \quad \mathbf{S}(x, p) = \frac{1}{4m} (E_p \varpi_S + \mathbf{p} \times \varpi_T),$$

where E_p , \mathbf{p} , m are the Λ 's energy, momentum, and mass, respectively. The spin vector of Λ in its rest frame is denoted as $S^{*\mu} = (0, \mathbf{S}^*)$ and is related to the same quantity in the c.m. frame by a Lorentz boost. Finally:

$$P = \frac{\langle \mathbf{S}^* \rangle \cdot \mathbf{J}}{|\langle \mathbf{S}^* \rangle| |\mathbf{J}|},$$

[F. Becattini et al, Phys. Rev. C 95, 054902 (2017)]

- Represents a Monte Carlo method for the time evolution of the various phase space densities of particle species.
- Based on the covariant propagation of all hadrons on classical trajectories, stochastic binary scatterings, resonance and string formation with their subsequent decay.
- Provides the solution of the relativistic Boltzmann equation.
- The collision criterion (black disk approximation):
$$d < d_0 = \sqrt{\sigma_{tot}(\sqrt{s}, \text{type})}/\pi$$
- 55 baryons and 32 mesons are included. All antiparticles and isospin-projected states are implemented.
- Cross sections are taken from PDG.
- Resonances are implemented in Breit–Wigner form.

[S. A. Bass et al, Prog. Part. Nucl. Phys. 41 (1998) 255-369,
M. Bleicher et al, J. Phys. G: Nucl. Part. Phys. 25 (1999) 1859-1896]

Statistical model

Input from UrQMD:

$$\varepsilon_{UrQMD} = \frac{1}{V} \sum_i E_i$$

$$\rho B_{UrQMD} = \frac{1}{V} \sum_i B_i$$

$$\rho S_{UrQMD} = \frac{1}{V} \sum_i S_i$$

Stat. Physics:

$$\varepsilon_{stat} = \sum_i \varepsilon_i(T, \mu_B, \mu_S)$$

$$\rho B_{stat} = \sum_i B_i n_i(T, \mu_B, \mu_S)$$

$$\rho S_{stat} = \sum_i S_i n_i(T, \mu_B, \mu_S)$$

$$\chi^2 = \frac{(\varepsilon_{UrQMD} - \varepsilon_{stat})^2}{\sigma_\varepsilon^2} + \frac{(\rho B_{UrQMD} - \rho B_{stat})^2}{\sigma_{\rho B}^2} + \frac{(\rho S_{UrQMD} - \rho S_{stat})^2}{\sigma_{\rho S}^2}$$

Minuit2 numerical minimizer

Output:
 T, μ_B, μ_S